Dear John,

You will see that I have responded to all the Reviewers' comments, below, and edited accordingly.

Additionally, because of removal of the old sections 2. Theoretical Background, I have provided a little bit of background in the new section 2 for the non-expert. Concerning the removal of the old section 3.1.1 Level Bottom, all references to this have been removed throughout the paper: in the discussion of both KdV and eKdV model results, the summary and conclusions, and a very slight change in the abstract.

Thanks and best wishes,

Kieran O'Driscoll

Response to Referee #1 comments

Kieran O'Driscoll would like to thank the reviewer for their considerable and thoughtful review.

Based on the general comments of Reviewer 1 (and also those of Reviewer 2):

Much of the material presented here in section 2 and 3 is well-known and does not need to be repeated here.

Likewise, the behaviour of internal solitary waves propagating over a slope has been widely studied in both the KdV and eKdV models, with often a main focus on polarity change when the coefficient of the quadratic nonlinear term changes sign.

The simulations with a linear bottom slope and with the topography of the Middle Atlantic Bight have some marginal interest in that most studies have examined the behaviour of a single solitary wave, rather than a developing wave train as here, although the outcome can be understood in terms of the known behaviour of a single solitary wave, namely adiabatic deformation and transition to an elevation solitary wave train riding on a negative pedestal when the usual transition is from a negative to positive coefficient.

The most interesting and novel part of the paper is section 4 where the model simulations are compared with observational data from the Middle Atlantic Bight. Although there have been several such comparisons in the literature for other sites, this would seem to be the first for this site. In summary I would recommend that the authors prepare a heavily revised and shortened paper which focusses on the material in section 4.

Response: Done. The article has been shortened by removing Sections 2 (Theoretical Background), 3.1.1. (Two-layer model level bottom), and Figs. 1 – 6.

Specific Comments:

(1) Further to the comments made above, in particular most of the text in section is not needed, and neither are figures 1-6.
Done, see above.

(2) The measure χ (10a) of the relative roles of nonlinearity and dispersion is unconventional and uninformative. A better measure is simply the ratio α/β, where it should be noted that in the KdV equation (1) division by β and a rescaling of time, clearly indicates that this is the effective measure of nonlinearity vis-a-vis dispersion.

Done. Removed with Section 2.

(3) The transition of the steepening front into a solitary wave train is best understood using the Whitham modulation theory and asymptotic solution, as developed by Gurevich and Pitaevskii. It is well known that, at least in the KdV model, the leading waves are solitary waves. The detailed discussion on this aspect is not needed here.

Done. The detailed discussion on this aspect has been removed with the old section 3.1.1 (previous version)

(4) The large-amplitude solitary wave solutions of the eKdV equation are more usually called “table-top” waves than the term “tanh” used in the text.

Done.

(5) The title should mention “internal” and should not use an acronym.
Done.

Response to Referee # 2 comments

Kieran O'Driscoll would like to thank the reviewer for their substantial and considerate review.

Based on the general comments of Reviewer 2 (and also those of Reviewer 1):

I have a number of problems with the paper and think that is requires significant revision. My basic problem is that there doesn't appear to be much that is new here other than the application to the CMO site in the Middle Atlantic Bight and that is quite a small part of the paper.

The paper needs considerable polishing. Figures are in some cases hard to read and many dimensional values are given without units. It would probably benefit from being shortened and more focussed on the comparisons with observations however I am not convinced of the value of these simulations in that context. The authors make some comparisons of their results with those of Holloway et al from 30 years ago. Recent work has been done in this area using model equations that include rotation (e.g., Grimshaw and co-workers). The authors need to make a compelling argument for this set of simulations.

Response: Done. The article has been shortened by removing Sections 2 (Theoretical Background), 3.1.1. (Two-layer model level bottom), and Figs. 1 – 6.

Comments

1. The title highlights KdV solutions with no mention of the eKdV solutions. I think it is well established by now that cubic nonlinearity is necessary to adequately model many observed solitary waves in the ocean, so if anything the eKdV equation should be mentioned in the title. Indeed, one wonders what the benefit of even considering the KdV equation is. Comparisons of the predictions of the KdV and eKdV (or Gardner) equations, as well as the RLW equation, with fully-nonlinear numerical simulations for a two-layer stratification are discussed in Lamb and Xiao (Ocean Modelling, 2014). This seems like a relevant reference.

Done, thanks.

2. Why are rotational effects not considered? The site of the observations is at mid-latitutude where rotation is going to affect the evolution of the internal tide and the amount of energy that ultimately gets transferred to ISWs. For example in Figure 10 the linear long wave propagation speed is about 0.5 m/s so waves take about 50 hours to travel 100 km. That is lots of time for rotation to affect their evolution.

The model is two-dimensional, so the waves propagate in the horizontal x-direction only and rotation is not included. This is stated in the abstract, discussion and summary.

3. First paragraph of page 4. Nonlinear effects can become important even without shoaling, as illustrated by the authors own flat-bottomed simulations so this should be reworded.

Done: Section 2 (Theoretical Background) has been removed

4. Page 5, lines 6–8. “It was originally developed in the context of internal waves by Benney ....”

Done: Section 2 (Theoretical Background) has been removed

5. Equations 10(b) and 10(c) are both incorrect.

Done: Section 2 (Theoretical Background) has been removed

6. Page 10. The introduction to section 3 repeats material from the introduction so should be deleted.

Done

7. Page 12, line 15: For a given water depth and wave amplitude cubic ...”. Then on lines 16–18, whether or not the eKdV model is similar to the KdV model depends a lot on the wave amplitude. For a two layer stratification, whenever the interface gets displaced close to the mid-depth cubic nonlinearity becomes important (though if h1/h2 << 1 higher-order nonlinear may be needed).

Done: Section 3.1.1 (Two-layer model level bottom) has been removed

8. Section 3.1.1. The cases explored in this section are not well explained. All four cases have different total depths H = h1 + h2 and different depth ratios h1/h2 while from what I can understand the initial wave amplitude is the same in all cases. So both the depth ratio h1/h2 and the initial nonlinearity have been changed. Comparing these cases is then a bit problematic, particularly with statements to the effect that you expect one case to be more nonlinear than the other. Also, throughout ratios such as α/c and β/c are given without units. These ratios are not dimensionless. The KdV and eKdV equation have been used a lot to model internal solitary waves in the ocean. What have we learned from this set of simulations?

Done: Section 3.1.1 (Two-layer model level bottom) has been removed

9. Section 3.1.2. What is new here? The general picture of the evolution of a shoaling internal tide has already been well described. What is the new contribution from this section?

These simulations studied the development of evolving internal tide as a packet or developing wave train across the linear sloping bottom, whereas most other studies have inspected the development and advance of a single soliton across similar bottom slope.

10. Page 17, Line 5: there are no higher-order terms to prevent the development of solitary waves in the models used here.

Sentence has been removed.

11. Page 18, lines 14–15: What do you mean by 'We expect the waves to become unstable"? Do you mean your numerical solution is unstable? If so should a smaller time step be used? If a physical instability what type of instability is referred to?

No, physically unstable, ie., Kelvin-Helmholtz instability or billows.

Done, thanks.

12. Page 19, line 14: Do you mean the CMO line will be horizontal — lots of straight lines don't have constant h1.

Yes, thanks. I will add Fig S1 (to replace old Fig 2) which shows values of h1, h2 for CMO.

<u>Note:</u> No need to add Fig S1 for this case, CMO parameter values are shown in Fig. 4a

13. Page 21, lines 9–10. α/α1 is not a dimensionless parameter.

Done, thanks. That was a typo, as seen from line 11, one line along. This section has now been removed.

14. Page 22, lines 3–8. Why is α1 so much greater at the CMO site than in case A? Is it because h1 is so much less?

Yes, thanks. Due to h1 half the value of h2. I have included Fig. S1 (α/α1) to show this. I have also included the equation: $\frac{\alpha}{\alpha_1} = 4\frac{h_1 - h_2}{h_1 h_2 (h_1{}^2 + h_2{}^2 + 6h_1 h_2)}$

while adding: , *where* h_1 *and* h_2 *are, respectively, twice and less than that at the CMO site. Done.*

15. Page 25, line 15. Do you mean figure 16c?

Yes, thanks.

16. Page 26, 2nd paragraph. Something else that could be going on is the nonlinear evolution of inertia-gravity waves that form behind internal solitary waves due to rotation. See Grimshaw et al, JPO, 2014 or Lamb and Warn-Varnas, NPG, 2015. What about multiple packets forming each tidal period because of different generation mechanisms or multiple tidal constituents?

Thanks, done. References to these papers and alternate generation and evolution processes included as follows:

Another possible generation mechanism is the nonlinear evolution of inertia-gravity waves forming behind internal solitary waves due to rotation, see further in Grimshaw et al. (2014) and Lamb & Warn-Varnas (2015). It is also possible that multiple packets form each tidal period, due to different generation mechanisms such as multiple tidal constituents or harmonics of a tidal components as found, for example, at the site of the Littoral Optics Experiment where the 4^{th} harmonic of the semi-diurnal tide was used to successfully simulate the evolution of the internal tide (O'Driscoll 1999).

17. Page 29, lines 8–9. The internal tide is nonlinear right from the beginning — it doesn't become nonlinear sooner as β is reduced. As β is reduced waves have to get narrower before dispersive effects become significant.

Yes, thanks. Done. Changed accordingly. This has been removed since it is concerned with Cases 1-4, flat bottom and old Fig. 1-6.

18. Page 29, line 16. I think you mean if this ratio is much larger than one

Yes, thanks. Done. Edited accordingly.

19. Page 30, line 8. What do you mean by 'the internal tide was forced with a sech2 wave. Don't you mean the simulation was initialized with a sech2 wave?

No. It is forced, since it takes a tidal period for the wave to propagate into the model domain, i.e. the sech2 wave has tidal period.

20. Figures. In general I find the font size too small in most of the figures – it is difficult to read them. In the caption for Figure 7 panels (a), (b) and (c) referred to in the text are not labeled. Figure 11 is of particularly poor quality

Done. Figures with problem font sizes have been increased in size (because of removal of Figs. 1-6). Fig. 7 relabelled, Fig. 11 removed.

Title page

Title: **Simulations and observation of nonlinear internal waves on the continental shelf: ~~KdV~~Korteweg-de Vries and extended Korteweg-de Vries solutions**

First Author: Kieran O'Driscoll
Second Author: Murray Levine*

First Author address:
Kieran O'Driscoll
School of Natural & Built Environment
Queen's University Belfast
email: kieran.odriscoll@qub.ac.uk
Tel: +44 (0)28 9097 4204
Fax: +44 (0)28 9097 4278

*deceased

Simulations and observation of nonlinear internal waves on the continental shelf: ~~KdV~~Korteweg-de Vries and extended Korteweg-de Vries solutions

Kieran O'Driscoll[1], Murray Levine*
[1]Department of Civil Engineering, Queen's University Belfast, Belfast, BT9 1NN, Northern Ireland
*deceased

Correspondence to: Kieran O'Driscoll (kieran.odriscoll@qub.ac.uk)

Abstract. Numerical solutions of the Korteweg-de Vries (KdV) and extended Korteweg-de Vries (eKdV) equations are used to model the transformation of a sinusoidal internal tide as it propagates across the continental shelf. The ocean is idealized as being a two-layer fluid, justified by the fact that most of the oceanic internal wave signal is contained in the gravest mode. The model accounts for nonlinear and dispersive effects but neglects friction, rotation, and mean shear. The KdV model is run for a ~~variety~~number of idealized stratifications and unique realistic topographies to study the role of the nonlinear and dispersive effects. In all model solutions the internal tide steepens forming a sharp front from which a packet of nonlinear solitary-like waves evolves. Comparisons between KdV and eKdV solutions is explored. The model results for realistic topography and stratification are compared with observations made at moorings off Massachusetts in the Middle Atlantic Bight. Some features of the observations compare well with the model. The leading face of the internal tide steepens to form a shock like front, while nonlinear high frequency waves evolve shortly after the appearance of the jump. Although not rank ordered, the wave of maximum amplitude is always close to the jump. Some features

of the observations are not found in the model. Nonlinear waves can be very widely spaced and persist over a tidal period.

1. Introduction

Internal waves are present throughout earth's oceans wherever there is stratification, from the shallowest near-shore waters to the deepest seas. Internal waves are important to physical oceanographers because they transport momentum and energy, horizontally and vertically, through the ocean, e.g. Munk (1981), Gill (1982). They provide shear to turbulence which results in energy dissipation and vertical mixing, e.g. Holloway (1984), Sandstrom & Elliott (1984). Biological oceanographers are interested because the internal waves carry nutrients onto the continental shelf and into the euphotic zone, e.g. Shea & Broenkow (1988), Sandstrom & Elliott (1984), and Holloway et al. (1985). They are of interest to geological oceanographers because the waves produce sediment transport on the shelf, e.g. Cacchione & Drake (1986). Civil, hydraulic and ocean engineers are interested because the internal waves generate local tidal and residual currents, e.g. Willmott & Edwards (1987), which can cause scour on nearshore as well as offshore structures, e.g. Osborne et al. (1978). Large nonlinear IWs are also of interest to the navy because they cause large vertical displacements and large vertical velocities that may affect underwater operations.

This study is focused on the internal tide and subsequent evolution of nonlinear waves. Internal waves in the ocean span the frequency spectrum from the buoyancy frequency, N, to the inertial frequency, f. However, the internal, or baroclinic, tide accounts for a large fraction of the energy contained

in these waves. The internal tide is generated by the interaction of barotropic tidal current with topography and not directly by the gravitational attraction of sun and moon. The properties and propagation of linear internal tide and waves have been treated in detail by many investigators, see, for example, Garrett & Munk (1979), or the monographs by Gill (1982), Lighthill (1978), or Apel (1987).

As the internal tide shoals, the nonlinear terms in the Navier-Stokes equations become important. These tidal waves of finite amplitude may evolve into packets of high frequency nonlinear waves. The equations describing these waves are much more complex than the linear equations and few mathematical solutions have been found.

We are interested in nonlinear internal waves because they are a very energetic part of the signal in time series that we have observed on continental shelves and in the shallow ocean. We are guided by numerical solutions of Korteweg-de Vries (KdV) type equations that incorporate both weak nonlinear and weak dispersive effects.

The state of the art on the evolution of internal solitary waves across the continental shelf is reviewed in Grimshaw et al. (2010). Grimshaw et al. (2004) simulated the transformation of internal solitary waves across the North West shelf of Australia, the Malin shelf edge, the Arctic shelf; Holloway (1987) discussed the evolution of the internal tide in a two-layer ocean on the Australian North West Shelf. Our model simulations of the evolution of the internal tide across ~~realistic in the~~ Middle Atlantic Bight topography ~~cases~~ are unique since these waves have never been modelled across such topography and stratifications, ~~but~~and the model results are compared with observations made at moorings off Massachusetts during the Coastal Mixing and Optics ~~Experiment.~~(CMO) Experiment. For the model cases of linear bottom sloping realistic topography, whereas most studies have focused on the behaviour

of a single soliton, this work is concerned with the development and evolution of a packet of solitary waves.

The goal of this paper is to study the observed variability in the evolution of the internal tide as it crosses the continental shelf resulting from different stratifications and varying topography.

In section 2, the model framework is presented, and model runs and results of simulations are discussed for cases of linearly sloping bottom topography and that at the site of the Coastal Mixing and Optics experiment (CMO). Model results are compared with data and observations collected at the CMO site in section 3. A summary and conclusions are presented in section 4.

~~The theoretical background of the Korteweg-de Vries (KdV) equation and an extended form of it, the eKdV, are presented in section 2. In section 3, the model framework is presented, and model runs and results of simulations are discussed. Model results are compared with data and observations collected at the site of the Coastal Mixing and Optics experiment (CMO) in section 4. A summary and conclusions are presented in section 5.~~

~~2. Theoretical Background~~

~~The Korteweg-de Vries (KdV)~~

2. ~~equation is well known to be a suitable physical model for describing weakly nonlinear advective effects and linear dispersion in internal waves. It was originally developed by Benney (1966) and extended to second order by Lee & Beardsley (1974). The KdV equation is derived from classical nonlinear long wave theory using a two-parameter perturbation expansion in ϵ and δ which scale the nonlinear and dispersive effects, respectively.~~

The KdV equation, derived following the procedure of Lee & Beardsley (1974) and the discussion by Lamb & Yan (1996), but without mean current, is given by

$$\eta_t + c\eta_x + \alpha\eta\eta_x + \beta\eta_{xxx} = 0 \qquad 1$$

where η is the vertical displacement amplitude of the wave mode, c is the linear long wave phase speed for the mode whose amplitude is η, α and β are coefficients of the non-linear and dispersive terms, while subscripts represent derivatives in time, t, and space, x, respectively.

Progressing to 2nd order in ε and δ (nonlinear and dispersive effects) yields four additional terms to Eq.(1) – a cubic nonlinear term, as well as higher-order linear and nonlinear dispersive terms – and is known as the fully-extended KdV equation (feKdV). Often only the second-order nonlinear term ('cubic nonlinearity') is added resulting in the extended KdV (eKdV) equation

$$\eta_t + c\eta_x + (\alpha + \alpha_1\eta)\eta\eta_x + \beta\eta_{xxx} = 0 \qquad 2$$

where α_1 is the coefficient of the cubic nonlinear term. In a two-layer model, for example, when the layers are of similar depth, or when the quadratic nonlinear term is small, the higher-order linear and nonlinear dispersive terms can be omitted, see discussion in Grimshaw et al. (2002). Continuous stratification can support an infinite number of modes. For simplicity we consider wave propagation in a two-layer stratification which supports one mode only. The justification for making this approximation is that most of the energy in the ocean appears to be contained in the first mode anyway, e.g. Alford & Zhao (2007) and discussion therein, while the shelf often has the appearance of a two-layer stratification: an upper mixed layer separated from a weakly stratified bottom layer by a thin pycnocline. This approximation greatly simplifies the problem; the numerical scheme is much less complex for the two-layer case than the continuously stratified case, and the results are easier to interpret. The coefficients of the KdV and

eKdV equations are greatly simplified for a two-layer fluid and are written (e.g. Ostrovsky & Stepanyants, 1989)

$$c = \sqrt{\frac{g\Delta\rho}{\rho}\frac{h_1 h_2}{h_1 + h_2}}; \qquad \alpha = \frac{3}{2}c\frac{h_1 - h_2}{h_1 h_2}; \qquad 3(a,b)$$

$$\beta = c\frac{h_1 h_2}{6}; \qquad \alpha_1 = -\frac{3c}{8h_1^{\,2}h_2^{\,2}}\left(h_1^{\,2} + h_2^{\,2} + 6h_1 h_2\right) \qquad 3(c,d)$$

where $\Delta\rho$ is the density difference between upper and lower layers, and h_1, h_2 are thicknesses of the two layers. We are interested in applying the KdV and eKdV equations to conditions of spatially varying coefficients. This problem has been investigated for slowly varying topography and stratification by Grimshaw (1979) and Pelinovsky et al. (1977). The eKdV equation then has variable coefficients and an additional term:

$$\eta_t + c\eta_x + (\alpha + \alpha_1\eta)\eta\eta_x + \beta\eta_{xxx} + \frac{c}{2Q}Q_x\eta = 0 \qquad (4)$$

where $Q = \frac{Mc^3}{M_0 c_0^{\,3}}$ and $M = \frac{h_1 + h_2}{h_1 h_2}$. 5(a,b)

and both c and M in Q vary in the horizontal direction, where the zero subscript indicates a constant value at a predetermined position. We note that the effective depth, h', is the inverse of the parameter M, Eq. (5b), contained in Q. For level bottom with horizontal interface the values of h_1 and h_2 are constant and Q=1 everywhere so the horizontal variability term vanishes, and the canonical KdV is the valid model. The variable coefficient KdV equation is the same as the variable coefficient eKdV equation but with $\alpha_1 = 0$. For convenience in solving the equation, we avail of a transformation, utilized by Pelinovsky & Shavratsky (1976), of the space and time variables x and t to variables l and s, respectively, given by

$$s = \int_0^x \frac{dx}{c(x)} \quad t, \quad l = x. \qquad 6$$

The transformed eKdV is then,

$$\zeta_l + \frac{1}{c^2\sqrt{Q}}(\alpha + \alpha_1\zeta)\zeta\zeta_s + \frac{\beta}{c^4}\zeta_{sss} = 0 \qquad 7$$

and

$$\zeta = \eta\sqrt{Q(l)}. \qquad 8$$

The transformation scales time so that disturbances traveling at the linear speed, c, remain at constant s. The system is often referred to as a slowness coordinate system. Because ζ varies relatively slowly in l/c compared to s, terms such as $c\zeta_{\xi}$ are neglected relative to $\zeta_{\xi\xi}$. The transformed KdV equation is the same as the transformed eKdV equation with $\alpha_1 = 0$.

Important solutions of the KdV and eKdV equations are waves of permanent form. One family of these waves are the solitary waves. There is a strong tendency for a long but otherwise arbitrary initial condition to evolve into a train of solitary waves (e.g. Lee & Beardsley, 1974; Drazin & Johnson, 1989). The solitary wave solution for the KdV equation in (l, s) space for constant parameters is given by (Zhou & Grimshaw, 1989)

$$\eta = \eta_0 \operatorname{sech}^2\left(\frac{\frac{c-V}{c}l + cs}{\Delta}\right) \quad \text{where} \quad V = c + \frac{\alpha\eta_0}{3}, \quad \Delta^2 = \frac{12\beta}{\alpha\eta_0}. \qquad 9(a, b, c)$$

The solitary wave is a single 'bump' propagating at speed V without change in form non-linearity being balanced by dispersion (Fig.1(a)). The amplitude, η_0, is inversely proportional to the square root of the

Formatted: Font color: Black, Kern at 16 pt

Formatted: Normal, Line spacing: Double

Formatted: Font: Italic

Formatted: Font: Italic

~~width, Δ – higher amplitudes imply narrower widths. The solitary waves can be either waves of elevation ($\eta_0 > 0$, $\alpha > 0$) or waves of depression ($\eta_0 < 0$, $\alpha < 0$). Since the product $\alpha\eta_0$ is always greater than zero, KdV solitary-like waves always travel with wave speed greater than c, Eq. (9b). For future use, it is useful to consider the difference between the magnitude of the nonlinear and dispersive terms:~~

$$\chi = \left|\frac{\alpha}{c^2}\eta\eta_s\right| - \left|\frac{\beta}{c^4}\eta_{sss}\right| \qquad \text{10 (a)}$$

~~and the analytical values of these terms for $\eta = \eta_0 \mathrm{sech}^2(\xi)$, where ξ is the argument given in Eq. (9a), are:~~

$$\frac{\alpha}{c^2}\eta\eta_s = \frac{2\alpha}{c\Delta}\eta\eta_0 \mathrm{sech}^2(\xi) \qquad \text{10 (b)}$$

$$\frac{\beta}{c^4}\eta_{sss} = 8\frac{\beta}{c\Delta^3}\eta_0\left(\mathrm{sech}^2(\xi)\tanh(\xi)\right)\left(2\mathrm{sech}^2(\xi) - \tanh(\xi)\right). \qquad \text{10 (c)}$$

~~Note that for $\mathrm{sech}^2(\xi)$ the nonlinear term is for the most part larger than the dispersive (Fig. 1(b)).~~

~~The solitary wave solution to the eKdV equation has a more complicated analytical form (Stanton & Ostrovsky, 1998):~~

$$\eta = \frac{\alpha\nu}{2\alpha_1}\left\{\tanh\left(\frac{\frac{c-V}{c}l + cs}{\Delta} + \sigma\right) - \tanh\left(\frac{\frac{c-V}{c}l + cs}{\Delta} - \sigma\right)\right\} \qquad \text{11(a)}$$

~~where ν is a nonlinearity parameter between zero and one, and the other parameters are~~

$$V = c\frac{\alpha^2\nu^2}{6\alpha_1}; \Delta^2 = -\frac{24\alpha_1\beta}{\alpha^2\nu^2}; \sigma(\nu) = \frac{1}{4}\ln\left[\frac{1+\nu}{1-\nu}\right]. \qquad \text{11(b,c,d)}$$

~~The shape of the 'tanh' eKdV solitary wave is similar to the 'sech^2' KdV solitary waves for small amplitude (Fig. 1c). As amplitude increases the eKdV solitary waves become thicker than the KdV solutions. Unlike the sech^2 solitary wave, the tanh wave has a maximum amplitude, which is given by α/α_1 (e.g. Stanton & Ostrovsky, 1998). For our application we assume sinusoidal tidal forcing at the boundary $l = 0$, Eq. (12a), where a_0 is tidal amplitude and ω is the frequency of the internal tide, with periodic conditions Eq. (12b)~~

$$\zeta(s, l=0) = a_0 \sin(\omega s) \qquad \zeta\left(s + \frac{2\pi}{\omega}, l\right) = \zeta(s, l). \qquad 12(a,b)$$

~~We employed the same finite difference scheme as Holloway et al. (1997) to solve the eKdV Eq. (7) numerically. The finite difference scheme is a central difference method, (e.g. Lapidus & Pinder, 1982), which was first developed for the KdV equation by Berezin (1987), and for the variable coefficients KdV by Pelinovsky et al. (1977). The difference scheme for the generalized KdV equation remains numerically stable provided~~

$$\frac{\Delta s}{\Delta l}\left(|\alpha\zeta| + \frac{3\sqrt{3}\beta}{2(\Delta l)^2}\right) < 1 \qquad 13$$

~~where Δl and Δs are grid resolution spacing values in space and time, respectively, (e.g. Holloway et al., 1997). Note values of Δs = 55s and Δl = 10 m are used throughout this work.~~

~~37.~~ Two-Layer Model

Formatted: No bullets or numbering

We are interested in modeling the evolution of the internal tide as it propagates shoreward from the shelf break. Since the greatest oceanic signal is the first internal mode, the stratification of the

continental shelf/slope region is modeled as a two-layer fluid. ~~-~~This approximation greatly simplifies the problem; the numerical scheme is much less complex for the two-layer case than the continuously stratified case, and the results are easier to interpret. ~~-~~Using ~~the two-layer~~this model configuration, we study the propagation of the internal tide over ~~various types of~~linear sloping and CMO topography~~,~~ ~~including the simplest case of flat bottom with level interface and progressing to realistic topography with sloping interface~~. All cases have been run within the quadratic nonlinear framework of the KdV equation, and the results are compared with an extended form of it, the eKdV model.

For the KdV Eq. (1) and eKdV ~~Eqs. (1,~~ Eq. (2) to be valid, the leading two terms must constitute the

$$\eta_t + c\eta_x + \alpha\eta\eta_x + \beta\eta_{xxx} = 0 \qquad (1)$$

$$\eta_t + c\eta_x + (\alpha + \alpha_1\eta)\eta\eta_x + \beta\eta_{xxx} = 0 \qquad (2)$$

primary balance.~~-~~ The nonlinear and dispersive terms can become important, but the assumptions leading to the KdV and eKdV equations are violated if either of the nonlinearity or dispersion terms approach the magnitude of the leading terms. Nonlinear transformation of the internal tide leads to the generation of nonlinear waves which tend to become solitary-like in form as the dispersive term becomes important.

~~We begin by discussing the coefficients of the KdV and eKdV equations for a two-layer fluid, where the density difference between the layers is chosen to be a constant: $g\Delta\rho/\rho$ = .014 m/s^2~~;Note, the KdV equation is well known to be a suitable physical model for describing weakly nonlinear advective effects and linear dispersion in internal waves. It was originally developed by Benney (1966) and extended to second order by Lee & Beardsley (1974). The KdV Eq. (1) and eKdV Eq. (2) equations are

Formatted: Font: Bold, Font color: Red

Formatted: Indent: First line: 0 cm

derived following the procedure of Lee & Beardsley (1974) and the discussion by Lamb & Yan (1996). The two-layer KdV model approximation is discussed in Grimshaw et al. (2002), and justified since most of the energy in the ocean appears to be contained in the first mode anyway, see e.g. Alford & Zhao (2007). The coefficients of the KdV and eKdV equations are greatly simplified for a two-layer fluid, e.g. Ostrovsky & Stepanyants (1989). The problem has been investigated for slowly varying topography and stratification by Grimshaw (1979) and Pelinovsky et al. (1977). An interesting reference is Lamb & Xiao (2014), who took a similar approach to ours, comparing predictions of the KdV and eKdV models, and also the RLW equation, with fully-nonlinear numerical simulations for two-layer stratification over selected topographies. See O'Driscoll (1999) for a full discussion of our experiments.

For all simulations the density difference between the two layers is chosen to be a constant: $g\Delta\rho/\rho = .014\ m/s^2$, a representative value for the Coastal Mixing and Optics (CMO) experiment (Levine & Boyd, 1999), for example at a mooring in the Middle Atlantic Bight located at 40.5°N, 70.5°W, and also in agreement with the stratification near the mooring location displayed in Barth et al. ~~(1998). The linear phase speed, c, is then a function of h_1 and h_2 only, Eq. (3a) and~~ (1998). ~~Fig. 2a, with values of c symmetric about the line $h_1 = h_2$, since the parameter for the effective or harmonic depth,~~

~~$$h' = \frac{h_1 h_2}{h_1 + h_2} \qquad 14$$~~

~~is contained within the phase speed (Apel, 1987) and lines of constant total water depth are perpendicular to the line $h_1 = h_2$. For a given total water depth, the speed is greatest when $h_1 = h_2$ and decreases as difference in layer thickness increases. Starting at a point on the line $h_1 = h_2$ and keeping the thickness of one of the layers constant, the speed of the wave decreases as the thickness of the other layer decreases.~~

The coefficient of the non-linearity term, α, is also a function of h_1 and h_2 only, Eq. 3b and Fig. 2b. The values of α/c are anti-symmetric about the line $h_1=h_2$, where $\alpha/c=0$. Starting at a point on the line $h_1=h_2$ and keeping the thickness of one layer constant, the value of $\alpha \to \infty$ as the thickness of the other layer decreases. The absolute value of α/c changes least rapidly when $h_1 \approx h_2$. When the thicker layer is larger than the thinner layer by at least a factor of 2-3, then α/c is relatively insensitive to the thickness of the thick layer, that is when $h_2 >> h_1$, then $|\alpha/c| \approx 3/2h_1$ and is not a function of h_2. α/c is also important since when multiplied by the amplitude, η, it represents the ratio of the nonlinear to the linear terms in the KdV Eq. (1).

The coefficient of the dispersive term, β, divided by c is also a function of h_1 and h_2 only, Eq. 3c and Fig. 2c, whose values are symmetric about the line $h_1=h_2$. The value of β/c for any given water depth is a maximum when $h_1=h_2$, values decrease as either of the layers becomes small. The interpretation of

Fig. 2c as a ratio of terms is complicated since, unlike Fig.2b, the derivatives do not cancel and the ratio cannot be simplified.

The coefficient of the cubic nonlinear term, α_1, when divided by c is also a function of h_1 and h_2 only, Eq. (3d) and Fig. 2d. α_1 is always negative and is symmetric around the line $h_1=h_2$, while for a given water depth the magnitude of α_1 is least when $h_1=h_2$. The value of $\alpha_1 \to -\infty$ as either one of h_1 or $h_2 \to 0$. It is also useful to calculate the ratio α/α_1, see O'Driscoll (1999). The relative importance of the quadratic to cubic nonlinearity is given by $\alpha/\alpha_1\eta$. For a given water depth cubic nonlinearity is most important when $h_1 \approx h_2$, i.e. when the magnitude of α is small. The magnitude of the quadratic nonlinear term is

~~much greater than that of the cubic nonlinear term when the water depth of one layer is much greater than the other and in this case the eKdV model is very similar to the KdV model.~~

~~3.7~~2.1 The Korteweg de Vries (KdV) Model solutions

Formatted: List Paragraph, Outline numbered + Level: 2 + Numbering Style: 1, 2, 3, … + Start at: 1 + Alignment: Left + Aligned at: 0 cm + Indent at: 0.63 cm

Using the KdV equation, we ~~first~~ investigate 42 cases with ~~level bottom for different combinations of h_1 and h_2. We then progress to~~ constant sloping bottom, ~~with both~~ horizontal and sloping interface~~. Finally, we~~, and finally make model runs with realistic topography at the ~~sites of the~~ CMO~~.~~

~~3.1.1 Level Bottom~~

Formatted: Indent: First line: 0.63 cm

~~We begin by studying the evolution of the internal tide over a level bottom, with level interface (h_1 and h_2 constant). This simple fluid arrangement is instructive when developing an intuitive feel for the generation and propagation of internal wave packets. A level bottom is also a good approximation for the continental shelf where the total water depth changes slowly in the horizontal. Four cases (Cases 1-4) using different layer thickness were selected to look at the effects of different relative magnitudes of α and β (Table 1). Case 1 (h_1=50m, h_2=150m) was chosen because these are reasonable values of upper and lower layer depth on outer continental shelves. Results are shown in Fig. 3a-b and Fig. 4a-c. A sinusoidal internal tidal amplitude of 5 m was used as the forcing at $l = 0$, Eq. 12. As it propagates, the internal tide steepens on the trailing edge or "back face" of the sine wave and a shock-like front forms at about $l \approx 50$ km. At this stage we also see the beginnings of undulations developing behind the shock-like front. By 75 km a pack of nonlinear solitary-like waves has begun to form. It is evident at 100 km that the solitary-~~

~~like waves of depression are rank ordered with the largest amplitude first. The first three waves at 100 km are compared with the sech^2 solitary wave form in Fig. 4a. Using the values of α, β and c, the shape of the solitary wave, Eq. (10), is determined by a single parameter, the amplitude, which is subjectively adjusted for best fit. The fact that the subjectively chosen sech^2 fits contain an arbitrary offset does not prevent the waves from being exact solutions to the KdV~~ site. For convenience in solving the equation ~~provided they propagate locally and at the local offset depth, as was shown by Zabusky & Kruskal (1965). The smaller amplitude trailing waves, Fig. 4b, appear more symmetric and sinusoidal in shape compared to solitary waves. Fig. 3b is a contour plot of displacement showing propagation of the internal tide in (l,s) space. The~~, we avail of a transformation ~~to s and l space results in a wave of speed c following a line of constant s. A solitary wave with phase speed $V > c$ will appear at smaller value of s for increasing l along the propagation path, i.e. will curve to the left as the tide progresses vertically up the plot along a maximum /minimum. The maxima and minima of the nonlinear waves travel at different speeds with the leading one (at smallest s) traveling fastest. Since a~~, utilized by Pelinovsky & Shavratsky (1976), of the space and time variables x and t to variables l and s, respectively, given ~~solitary-like wave may vary in amplitude as it propagates in l, we also expect the track of the wave to curve in s and l space. The trailing sinusoidal-like waves travel with wave speed less than c, indicating that dispersion is important. An interesting observation is that some of the minima of the nonlinear waves initially travel with wave speed less than c and eventually travel with speeds greater than c (for example see 7th min. in Fig.3b).~~ by

$$s = \int_0^x \frac{dx}{c(x)} - t, \quad l = x. \qquad (3)$$

The transformed eKdV is then

$$\zeta_l + \frac{1}{c^2\sqrt{Q}}(\alpha + \alpha_1\zeta)\zeta\zeta_s + \frac{\beta}{c^4}\zeta_{sss} = 0 \qquad 4$$

where $\zeta = \eta\sqrt{Q(l)}$, $Q = \frac{Mc^3}{M_0 c_0^{\,3}}$, $M = \frac{h_1 + h_2}{h_1 h_2}$, and 0 subscripts represent initial values. The transformation scales time so that disturbances traveling at the linear speed, c, remain at constant s. The system is often referred to as a slowness coordinate system. Because ζ varies relatively slowly in l/c compared to s, terms such as $c\zeta_l$ are neglected relative to ζ_s. The transformed KdV equation is the same as the transformed eKdV equation with ~~Fig. 4c shows the difference between the magnitudes of the nonlinear and dispersive terms, χ (Fig.1b), for Case 1 at various distances in l. At 100km we see the balance changing over the tidal period. The leading waves at the left have the shape expected for a sech^2 solitary wave (Fig. 4a). The trailing waves to the right appear more sinusoidal in shape, and are relatively more dispersive than a sech^2 wave. Upwards of twenty waves have formed when the internal tide has traveled 160 km. The leading six to seven waves travel with speed greater than c and have a nearly sech^2 form. The trailing waves travel slower than c as expected for waves that are more dispersive.~~

~~For Case 2 we choose h_1 and h_2 such that $\alpha/c = .02$ as in Case 1, but the value of β/c is less than half that of Case 1. Since the ratio of the dispersive coefficient to the nonlinear coefficient has been reduced by more than half, we expect Case 2 to be more nonlinear, the internal tide to steepen sooner, and nonlinear internal waves to form at smaller l. Fig. 5 shows that the internal tide evolves similarly to Case 1. However, as expected, the shock-like front and subsequent undulations appear sooner (smaller~~

Formatted: Font color: Black, Kern at 16 pt
Formatted: Normal, Line spacing: Double
Formatted: Font: Italic
Formatted: Font: Italic

~~values of l). Comparing Figs. 3a and 5a, the internal tide is more nonlinear at l = 50 km for Case 2 than it is for Case 1, while a greater number of solitary waves have formed in Case 2 by l=100km, and are more closely spaced. More of the leading waves have sech^2 form at 165 km in Case 2 when compared to Case 1. For Case 2, a few more of the leading waves travel with speed greater than c compared with Case 1; the remaining waves have speed less than c, and disperse from the leading waves as l increases.~~

~~For Case 3 we choose β/c = 1250, as in Case 1, but with α/c = –.0021, a factor of ten less than the value used in Case 1 and 2. As a result, we expect the internal tide to be much less nonlinear. Indeed, the internal tide steepens slowly and even by l = 200 km solitary-type waves have not been generated (see O'Driscoll 1999).~~

~~For Case 4 the nonlinearity parameter is half that used in Case 1, α/c = –.01 and β/c is the same value. So, we expect the resultant internal tide to be more nonlinear than Case 3 but less so than either of Cases 1 or 2. The internal tide steepens slowly and the first wave of depression begins to form when $l \approx$ 100 km (Fig. 6). Fewer nonlinear waves have formed at this point than in either Case 1 or Case 2. By l = 200 km only two or three solitary-like waves have formed.~~

~~**3.1.2**~~$\alpha_1 = 0$. See O'Driscoll (1999) for further details.

2.1.1 Constant Bottom Slope

The propagation of the internal tide along constant sloping topography was studied for cases of constant upper layer thickness (Case A) and sloping interface (Case B), both of which are possible on continental shelves. We ~~have chosen~~chose starting layer thickness at ~~l=0 the same as Case 1 for a flat~~

bottom, i.e. h_1=50m $l = 0$ $h1 = 50m$ and h_2 =150m $h2 = 150m$, with bottom slope of 1/1000 $1/1000$ so that total depth decreases from 200$200$ to 0 m0 m over a distance of 200 km. $200\ km$.

We first investigate the case of constant sloping bottom with constant upper layer thickness (Case A). The value of c decreases in shallow water, while $\alpha \to 0 \alpha \to 0$ as $h_2 \to h_1 h_2 \to h_1$ at water depth of 100 m (Figs. 2, 7a).$100\ m$ (Fig. 1a). Seaward of this depth, where $h_2 > h_1, \alpha < 0 h_2 > h_1, \alpha < 0$ and solitary waves are waves of depression, whereas shoreward of this depth ($h_2 < h_1), \alpha > 0 h_2 < h_1,), \alpha > 0$ and solitary waves exist as waves of elevation only. $\beta \to 0 \beta \to 0$ as the product $h_1 h_2 \to 0$. Since $h_2 h_1 \to 0$. As the magnitude of $\alpha \alpha$ is initially relatively large we expect the sinusoidal internal tide to transform rapidly resulting in the formation of several nonlinear waves (as previously seen for the flat bottom cases). Since $\alpha \to 0$. Since $\alpha \to 0$, these waves may not be so nonlinear as to violate the weakly nonlinear constraint on the KdV model. However, sincebecause the value of α rapidly increases for l>100km, we expect the waves of elevation to become highly nonlinear thereby possibly violating the weakly nonlinear condition.

Figs. 7b1b and c show the internal tide signal for Case A at different values of l, i.e. and also at different water depths. The internal tide steepens and rapidly becomes nonlinear, resulting in the generation of a shock-like front and subsequent undulations by $l \approx 50 km l \approx 50 km$. Shoaling further, the internal tide becomes more nonlinear with the oscillations starting to resemble solitary waves by $l = 70 km l = 70 km$. However, unlike Cases 1, 2, and 4, the waves never develop into mature internal solitary waves assince the magnitude of α continually decreases. By $l = 90 km l = 90\ km$ the waves resemble a symmetric, dispersive packet, as further evidenced by Fig. 8a2a. Initially the relatively large

magnitude of ~~α~~ α resulted in the rapid steepening of the internal tide~~, so much so that the Case A tidal signal at l=50km resembles those of both Case 1 and Case 2 for flat bottom.~~. However, as the value of ~~$\alpha \to 0$~~ $\alpha \to 0$ the nonlinear waves are prevented from developing into solitary waves, since higher order terms (neglected in KdV) become of order α or larger and thus cannot be ignored, thereby rendering the KdV model invalid in this neighborhood. ~~-~~At ~~l=100km~~ $l = 100km$ the packet certainly looks symmetrical about a horizontal axis, that is to say the waves are neither polarized as waves of depression nor elevation, since KdV solitary waves cannot exist when ~~$\alpha = 0$~~ $\alpha = 0$. At ~~115km~~ $115km$ the waves have switched polarity; they have become waves of elevation, a result of α having become positive. This transition is seen in Fig.~~8b~~2b where the leading waves are compared with sech^2 solitary form. Beyond ~~100km~~ $100km$ the waves rapidly approach solitary waves of elevation since α becomes large quickly.

As the internal tide propagates into shallow water the leading face of the wave steepens but~~, unlike cases 1-4,~~ the decreasing magnitude of ~~α~~ α causes this steepening to slow down and there is virtually no change in wave slope steepness between ~~70~~70 and ~~90 km.~~ $90\ km$. The rate of change of the slope of the leading face changes sign when ~~α~~ α becomes positive and the slope steepens rapidly, while the back face of the internal tide slackens. The steepening of the leading wave will lead to the formation of a second shock-like front (or a "reverse hydraulic jump" as has been described by Holloway et al., 1997). Fig. ~~7c~~1c gives a clear picture of the wave speed~~. The~~: the leading solitary-type wave initially travels with speed very slightly greater than c but becomes slower than c when ~~$l \sim 90$km~~ $l \sim 90km$. The second solitary-type wave also has initial speed greater than c but becomes slower than c ~~when $l \sim 80$km.~~at $l \sim 80km$. All of the other waves travel with phase speed less than c. For ~~values of $l > 100$km~~ $l > 100km$ all waves travel

with speed less than *c*, the reason becomes clear upon examination of Fig. ~~8a~~2a which plots the difference between the magnitudes of the nonlinear and dispersive terms ~~for Case A~~.

The leading waves are slightly more nonlinear than dispersive when ~~$l \approx 70$ km~~ $l \approx 70\ km$ but become less so as *l* approaches ~~100 km~~$100\ km$. When ~~$\alpha = 0$ ($l = 100$km)~~ $\alpha = 0$ ($l = 100km$) the value of the nonlinear term is zero and the waves look like a dispersive packet. Since ~~$\alpha > 0$~~ $\alpha > 0$ for *l* ~~> 100 km~~ > $100\ km$, the nonlinear term is again a factor and the waves become a hybrid by ~~$l = 115$km~~ $l = 115km$, interchanging back and forth across the length of the wave between being more nonlinear and dispersive. The waves travel slower than *c* since the magnitude of the dispersive term is slightly greater than the nonlinear term.

For Case B with constant sloping bottom and sloping upper layer, we also begin in ~~200m~~$200m$ water with ~~$h_1 = 50$m and $h_2 = 150$m. For~~ $h_1 = 50m$, $h_2 = 150m$. In this ~~case~~instance the bottom slope is again ~~1/1000~~$1/1000$ and the interface slope is ~~1/4000 with the result~~$1/4000$ such that both layers vanish simultaneously at ~~200 km. The~~ $l = 200\ km$. KdV parameter values ~~of the KdV parameters~~ are shown in Fig. ~~9a~~3a. The magnitude of ~~α~~ α increases from ~~$l = 0$~~ $l = 0$ all the way to the shallowest water, unlike Case A where ~~α~~ α passes through zero, so we expect the internal tide to become nonlinear sooner than for Case A, and any solitary waves to remain as waves of depression. We do, however, expect the waves to become ~~unstable,~~physically unstable, leading to a Kelvin-Helmholtz instability (see e.g. Cushman-Roisin & Beckers 2011), a result of the increasing magnitude of the nonlinear parameter combined with the decreasing value of the dispersive parameter. This combination of events will result in the weakly nonlinear, dispersive KdV becoming invalid at ~~$l = 95$ km~~ $l = 95\ km$. Fig. ~~9b~~3b is a plot of the internal tide for Case B at several values of *l*. The internal tide steepens rapidly and a shock-like wave, followed

by undulations, has evolved from the transforming tide by ~~l=40km~~$l = 40km$. The internal tide continues to steepen and several nonlinear waves have formed by ~~l=55km~~$l = 55km$. These leading nonlinear waves mature into rank ordered solitary waves by ~~65km~~$65km$. Fig. ~~9c~~3c shows that most of the solitary waves eventually travel ~~at a~~with phase speed greater than c. The waves are more nonlinear than dispersive and the increasing value of the nonlinear parameter combined with the diminishing value of the dispersive parameter leads to the model becoming numerically unstable (O'Driscoll 1999).

~~3~~2.1.~~3~~2 Realistic topography and stratification

~~We now proceed to the transformation of the internal tide for the case of realistic topography for the CMO site.~~

The CMO site was located in the Middle Atlantic Bight. CTD profiles were made across the continental shelf from shallow water to beyond the continental slope. Boyd et al. (1997) have concluded that the internal tide at the site is primarily a first mode internal wave, further justifying our choice of a two-layer model. An upper layer thickness of ~~25 m~~$25\ m$ is a representative average value for the duration of the experiment (July and August 1996). ~~The line 'CMO' in Fig.2 shows the values that the KdV parameters take as the internal tide propagates across the continental shelf. Since the upper layer, h_1, is constant, the 'CMO' line will be straight, but since the total depth does not vary linearly in l, the value of h_2 does not change linearly along this line.~~

Fig. ~~10a~~4a shows ~~the~~KdV parameter values ~~of the KdV parameters~~ as a function of l. ~~-~~ Though undulating, the bottom topography is similar to the constant sloping bottom cases. Recall that we chose an upper layer depth of 50 m for Case A, whereas here we have chosen h_1 = 25 m. α starts out negative

Formatted: Font: Bold
Formatted: Indent: First line: 0 cm
Formatted: Indent: First line: 0 cm
Formatted: Font: Bold
Formatted: Font: 12 pt, Bold
Formatted: Indent: First line: 1.27 cm

with relatively large magnitude. The magnitude decreases, similar to Case A, changing sign as the bottom shoals and $h_1>h_2$ when the value increases rapidly. Values of β, c and the horizontal variability parameter, Q, are similar to Case A. Figs. ~~10b~~4b and c show results for tidal forcing of amplitude 2 m at 180 m water depth. The internal tide evolves similarly to Case A. ~~-~~A shock-like front has formed on the back-face of the internal tide at ~~l=40km~~$l = 40km$. Several nonlinear waves have formed by ~~l=60km~~$l = 60km$ (mooring location) with the leading ~~4-5~~$4 - 5$ waves appearing like solitary waves of depression and the trailing waves looking more like a dispersive packet. Several more waves have formed by ~~80km~~$80km$ but the number of solitary-like waves seems to have been reduced to the leading two waves. ~~-~~All of the trailing waves do appear as a dispersive packet since the magnitude of α has decreased. ~~-~~More waves continue to form but by ~~100 km~~$100\ km$ the packet is neither a pack of waves of elevation nor depression, not unlike Case A. Beyond ~~l=125km,~~$l = 125km,$ α becomes large ~~α,~~ the waves reverse polarity and rapidly develop into mature solitary waves of elevation. The results show that the CMO case and Case A are similar, though more solitary waves have formed for the CMO case, due to the fact that at the CMO site the value of ~~α~~α is initially twice that of Case A. The internal tide becomes unstable beyond ~~l=130km~~$l = 130km$, a result of the increasing value of the nonlinearity parameter combined with the vanishing dispersion parameter. Fig. ~~10c~~4c is a plot of the evolution of the internal tide as it propagates over the continental shelf, increasing in l. The leading solitary-like waves initially travel with speed very slightly greater than c, as in Case A. The waves slow down to travel at speed c where ~~l≈90km~~$l \approx 90km$ and α is very small. ~~The~~Wave speed ~~of the waves~~ then becomes slightly slower than c but faster and more complicated than Case A, due to the undulating topography.

The difference in magnitudes of the nonlinear and dispersive terms, ~~χ~~ $\chi = \left|\frac{\alpha}{c^2}\eta\eta_s\right| - \left|\frac{\beta}{c^4}\eta_{sss}\right|$, is plotted in Fig. ~~11.~~ 5. The leading 2-3 three waves are initially more nonlinear than dispersive but the diminishing magnitude of ~~α~~α leads to the waves becoming more dispersive-like and the waves begin to slow down. The negligible value of α between ~~l=100-115km~~$l = 100 - 115\ km$ results in the waves ~~behaving~~acting very much like a dispersive packet and they travel with wave speed slightly less than c. The increasing value of α after it passes through zero, leads to the nonlinear term becoming almost the same order of magnitude as the dispersive term before the model becomes numerically unstable shortly beyond ~~l=130km~~$l = 130\ km$.

~~3~~2.2 The extended Korteweg - de Vries (eKdV) model

~~All of the~~The model runs discussed in section ~~3~~2.1 were also made ~~using~~with the ~~extended Korteweg-de- Vries (~~eKdV~~)~~ equation. The ratio of the nonlinear parameters, ~~α/α_1~~, $\frac{\alpha}{\alpha_1} = 4\frac{h_1 - h_2}{h_1 h_2 (h_1^{\,2} + h_2^{\,2} + 6h_1 h_2)}$ (see e.g. Ostrovsky & Stepanyants, 1989) is the theoretical maximum amplitude for the solitary wave solution to the eKdV ~~solution~~equation. The ratio of the quadratic to cubic nonlinear terms in ~~the eKdV~~this equation depends upon ~~the~~ displacement height, ~~η~~ η_s and is given by ~~$\alpha/(\alpha_1\eta)$. For flat bottom, Cases 1, 2 and 4, the maximum amplitude η_0 ~18m for the KdV numerical solution.~~ $\frac{\alpha}{\alpha_1 \eta}$.

Formatted: Font: Not Italic

For Case ~~1, α/α_1 > 40 and therefore the nonlinearities result predominantly from the quadratic nonlinear term, see O'Driscoll (1999). For Cases 2 and 4 the magnitude of α/α_1 is just over 20 m, and both the quadratic and cubic nonlinear terms will be important.~~

~~For the case of sloping bottom with horizontal interface, Case~~ A~~,~~ the ratio ~~α/α_1 passesthrough~~ $\frac{\alpha}{\alpha_1}$ passes through zero (~~$h_1=h_2$~~)$h_1 = h_2$) and we expect the cubic nonlinear term to be important. The results of this model run are shown in Fig. ~~12~~6. The internal tide evolves similar to the KdV case (Fig. ~~7b~~1b) with a shock-type wave followed by several nonlinear oscillations on the back face of the internal tide at ~~l=50km~~$l = 50km$. The internal tide in both frameworks look similar at ~~70 km~~$70\ km$ where several nonlinear waves of depression ~~having~~have been formed. The KdV solitary-like waves flip polarity at ~~100 km~~$100\ km$ due solely to the fact that ~~α~~α changes sign there.

For the CMO case, comparison of KdV and eKdV ~~models~~results shows a more significant difference than for Case A. Fig. ~~13a~~7a-c ~~shows~~show the KdV and eKdV model results for a ~~4m~~$4m$ internal tide having propagated 60 km to a water depth of 69 m. The leading KdV model solitary wave (solid line) arrives at the CMO central mooring ~~~0.1~~~ 0.1 tidal period ahead of the leading eKdV model solitary wave (broken line). The KdV and eKdV models are so different at the CMO site when compared to Case A because the magnitude of ~~α_1~~α_1 is greater at the CMO site. Though the magnitude of ~~α~~α is less in Case A, the fact that the magnitude of α_1 is so small when compared to α means the addition of the cubic nonlinear term does little to change the KdV results. This is not true at the CMO site where the greater magnitude of α_1 is the reason for the difference between the KdV and eKdV frameworks, particularly as the internal tide propagates into shallower water and the magnitude of the ratio ~~α/α_1~~ $\frac{\alpha}{\alpha_1}$ is

Formatted: Font: Not Italic, Not Superscript/ Subscript

Formatted: Font: 16 pt

much greater for Case A, where h_1 and h_2 are, respectively, twice and less than that at the CMO site. Comparing the leading waves from the eKdV and KdV solutions reveals a fundamental difference in wave form; the KdV waves are taller and thinner (Fig. ~~13c~~7c). Solitary type solutions to the KdV (sech^2) and to the eKdV (tanh, also known as 'table-top' waves) are fitted to the leading waves (Fig. ~~13d~~7d-e). The leading wave in the KdV model is very well approximated by a sech^2 wave. ~~-~~The lead wave in the eKdV model is neither well approximated by sech^2 or ~~tanh~~table-top wave, but appears to be a hybrid between the two. Fits of sech^2 and ~~tanh~~table-top waves were made by subjectively choosing values of ~~η_0~~η_0 and ~~υ~~υ, respectively, while using the value of KdV and eKdV parameters for ~~69m~~$69m$ water depth. Note that the amplitude of the ~~tanh~~table-top wave is limited to ~~α/α_1~~$\frac{\alpha}{\alpha_1}$. Increasing ~~υ~~υ only serves to make the waves wider once ~~the~~its value ~~of υ~~ is close to one (~~Fig. 1c). The amplitude~~see e.g. O'Driscoll 1999). Amplitude and width of the leading waves ~~of~~in the packet are also compared in Fig. ~~14a~~8a. The width is defined as the time it takes the wave to pass a fixed point, as measured at ~~42%~~42% of the amplitude. Results from a range of different tidal amplitudes are also shown. For reference, the dotted lines represent sech^2 and ~~tanh~~table-top waves for the local values of parameters h_1, h_2, and $g\Delta\rho/\rho$. For KdV the leading wave of the ~~2m~~$2m$ tide always has amplitude greater than the second and the amplitudes of subsequent waves decrease in a rank ordered fashion. The leading wave is slightly thicker than the trailing ones which are all approximately equal in width. ~~-~~For the eKdV the leading wave has larger amplitude and is thicker than the trailing waves. For the KdV model with ~~4m~~$4m$ amplitude tide all the waves fall on the same spot on the sech^2 curve. For the eKdV model with ~~4m~~$4m$ amplitude tide, the waves appear on the 'thick' side of the sech^2 curve with the lead wave the most removed from the KdV

Formatted: Font: +Body (Times New Roman)

Formatted: Font: +Body (Times New Roman)

theoretical curve. The same is true for amplitudes of 5m and 6m. The eKdV model waves appear to be evolving toward the theoretical eKdV 'tanh' curve. Note that the amplitude of many of these waves ~~exceeds~~exceed the maximum amplitude of table-top/tanh ~~wave~~waves of ~~9 m~~9 m as determined by the local parameters at the CMO site.

Formatted: Font: Not Italic

To learn more about the evolution of a sine wave to waves with sech^2 and ~~tanh~~table-top form, we ran the model with constant parameters (flat bottom) using values at the mooring site. The runs were made with initial tidal amplitudes of 1, 2 and 4 m in both KdV and eKdV frameworks and the width vs. amplitude for the first and second wave in each packet is plotted at various increments of l (Fig. ~~14b~~8b). The KdV waves grow in amplitude with approximately constant width before turning to hug the theoretical KdV line. They then decrease in amplitude while increasing slightly in thickness. Though the KdV model waves continue to evolve, most of them can be well approximated as being 'sech^2' waves after ~~~100km (as was previously shown for Case 1 and Case 4).~~$\sim 100km$. For the eKdV case, the waves are initially close to the theoretical sech^2 KdV curve. The waves move slowly towards the theoretical eKdV tanh curve, ultimately decreasing in amplitude and increasing in thickness. The last points have been plotted after the internal tide has propagated ~~~240km~~$\sim 240km$. It appears that these waves are evolving toward ~~tanh~~table-top form, but mature over a relatively long distance. Also, the amplitudes of the waves are greater than the theoretical eKdV maximum but their magnitudes decrease as the tide evolves.

Another investigation to explore the evolution in the eKdV model (constant parameters) was made using an initial condition of a sech^2 wave, the solitary wave solution to the KdV equation. ~~Sech^2~~sech^2 amplitudes of 4m, 7m, 9m, and 13m (Fig. ~~14c~~8c) were chosen. The sech^2 waves are rapidly transformed

to ~~tanh~~table-top waves, e.g. the 4 examples plotted reach the theoretical eKdV curve after the wave has propagated about ~~10 km~~10 *km*. A solitary $sech^2$ wave evolves much more rapidly to ~~the tanh~~table-top form (Fig. ~~14c~~8c), as opposed to when it is part of a packet of waves (Fig. ~~14b~~8b). The reason for this has not been thoroughly investigated, but provides caution for treating a packet as a group of non-interacting waves.

~~38.~~3. Observations of Nonlinear Internal Waves

The data to be presented and discussed was collected during the CMO, for location see Fig. ~~15~~9. The CMO experimental field program was conducted to increase our understanding of the role of vertical mixing processes in determining the mid-shelf vertical structure of hydrographic and optical properties. The field program was conducted on a wide shelf so as to reduce the influences of shelf break and nearshore processes. The data we discuss was collected from the CMO Central Mooring in July and August 1996, a time when a strong thermocline is present as a result of large-scale surface heating, Boyd et al. (1997).

~~43~~.1 Observations during the Coastal Mixing and Optics Experiment

The Central Mooring of the CMO experiment was located at 40° 29.50' N 70° 30.46' W in water depth of ~~69 m~~69 *m*. A total of 24 temperature recorders and 5 conductivity sensors were distributed along the mooring. Currents were measured at 14 depths from an ADCP placed a few metres above the bottom.

Boyd et al. (1997) have calculated the first mode internal wave amplitude from the velocity time series for the period 29 July to the 31 August 1996 (year day 210 - 245, Fig. ~~16a).~~10 i)). The dominant

Formatted: List Paragraph, Numbered + Level: 1 + Numbering Style: 1, 2, 3, … + Start at: 3 + Alignment: Left + Aligned at: 0.63 cm + Indent at: 1.27 cm

barotropic tidal signal in the Middle Atlantic Bight is semi-diurnal, and is strongest over the period day 241-245 during spring tide (Fig. ~~17).~~ 11). A semi-diurnal signal is apparent in the first mode record, particularly during the spring tide period. A spectrum of the first mode amplitude (Fig. ~~18~~12) shows energy peak at both low and high tidal frequencies. Much of the high frequency energy is due to bursts or pulses of high frequency nonlinear internal waves that occur for a short period during the semi-diurnal tidal cycle. These nonlinear internal waves propagate shoreward across the continental shelf to the south of Martha's Vineyard. ~~-~~The energy at high frequency is greater over the period day 241-245 during spring tides (Fig. ~~18~~12). There is a clear maximum in energy at 2 cpd over this period, and a significant amount of energy is also contained at 4 cpd. The energy rapidly drops for frequencies greater than 4 cpd but there is a significant increase in energy at ~~~50 cpd~~$\sim 50\ cpd$ and ~~at ~90 cpd~~$\sim 90\ cpd$. To help interpret these observations, we compare them with the two-layer eKdV model using the CMO parameters. Since we do not know where the internal tide is generated or its amplitude, the model was run assuming a sinusoidal internal tide at distances of ~~24 km, 48 km~~$24\ km, 48\ km$ and ~~60 km~~$60\ km$ seaward of the mooring site. Three initial amplitudes of ~~2 m, 4 m~~$2\ m, 4\ m$ and ~~6 m~~$6\ m$ were used at each distance. Fig. ~~14c~~10 iii) shows the internal tide as it appears at the CMO mooring site for these nine cases. In all ~~cases~~instances, the leading face of the periodic sinusoidal wave slackens (or flattens) as the internal tide propagates shoreward. ~~-~~This is followed by a steepening of the back face which develops into a shock-like front.~~-~~ The shock-like front is followed by oscillations which subsequently evolve into a packet of solitary-like waves.

This same pattern can often be seen in the observed time series of the first internal mode. ~~-~~Fig. ~~19~~13 shows several individual jumps at the CMO mooring. Fig. ~~19a (~~13 i) (top left panel) shows first

modes which best match the model results of Fig.~~16c.~~10 iii). Some features of the observations compare well with the model. The slackened leading face of the tide is always followed by a steep - almost shock like - front followed by several highly nonlinear short period waves. Although not rank ordered, the largest amplitude wave in the observed packet is always at or near the jump. The model results show that the amplitude of the jump is greater for larger initial condition, and decreases with distance from the point of generation. Although nonlinear waves continue to evolve, their amplitudes decrease as they propagate shoreward from their generation point, and they become 'thicker', i.e. they become more ~~tanh~~table-top like. Though the modelled waves have amplitudes less than the theoretical tanh limit for local eKdV parameters, they nonetheless fit the shape of several observed waves at the CMO site.

There are also features of the observations that are not found in the model. Fig. ~~19 (~~13 i) top left ~~panel~~ (f) and (g) differ in that the packet that follows the shock-like front, persists until the end of the tidal period, and the waves are spread apart from each other. Fig. ~~19 (~~13 i) top left ~~panel~~ (c) shows two packets of solitary-like waves propagating past the mooring site over a tidal period. The leading slackened face is followed by a shock-like front and a packet of solitary waves. The trailing face then slackens to assume a slope similar to the leading face but a second shock-like front, followed by a packet of solitary waves, passes before the end of the tidal period. This could be from a second internal tide front coming from another generation site, there can be overlapping semi-circles of internal wave fronts from multiple generation sites, see for example discussion in Apel et al. (1988). Another possible generation mechanism is the nonlinear evolution of inertia-gravity waves forming behind internal solitary waves due to rotation, see further in Grimshaw et al. (2014) and Lamb & Warn-Varnas (2015). It is also possible that multiple

Formatted: Font: +Body (Times New Roman)

packets form each tidal period, due to different generation mechanisms such as multiple tidal constituents or harmonics of a tidal components as found, for example, at the site of the Littoral Optics Experiment where the 4th harmonic of the semi-diurnal tide was used to successfully simulate the evolution of the internal tide (O'Driscoll 1999).

Another common observation that is not found in the model results is a 'drop' in amplitude before the jump that occurs at the beginning of the wave packet. Fig. ~~19 (~~13 top left ~~panel (~~h) shows that the first internal mode drops between day 243.5 and 243.6 but the slackening slope is restored before the arrival of the jump and packet of solitary waves. Similar 'drops' also occur in Fig. ~~19 (~~13 top left ~~panel (~~b) and (e) and ~~(middle panel~~ top right (a) and (i). Another phenomenon observed is that the slope of the leading face of the tide changes sign before the packet in several of the examples in Fig. ~~19 (middle panel).~~13 top right. In Fig. ~~19 (middle panel~~ 13 top right (h) the low frequency slope changes sign at day 236, and the solitary waves appear as usual ahead of the trailing, low frequency signal. The signal becomes even more complicated when both a 'drop' and low frequency slope change are present, e.g. Fig. ~~19 (middle panel~~ 13 top right (d). In this case, the slope of the leading slackening low frequency signal changes sign at day 242.5 and is followed by a packet of four solitary waves. The low frequency signal is restored before the passage of a jump followed by a packet of five large solitary waves. The trailing face retains the slope of the low frequency signal. Fig. ~~19 (right panel)~~13 bottom shows a series of jumps which are more complex than those in the ~~left and center~~top panels, though they retain the basic structure of the model results over the tidal period.

To examine the details of the wave packets themselves, the width vs. amplitude was estimated for each wave from all events during the period day 210-245 (Fig. ~~20~~14). These waves are plotted along with the leading two waves from six of the nine model runs shown in Fig. ~~16c.~~ 10 iii). Also shown are the theoretical relations for solitary waves for the eKdV and KdV equations using CMO site parameters. The observed nonlinear waves vary greatly in amplitude and width, generally having amplitudes of ~~between 5 and 25~~$5 - 25$ metres, and widths of ~~between 200 and 600~~$200 - 600$ seconds. Larger amplitude observed waves are well approximated by model runs with large initial amplitude, particularly the ~~4m~~$4m$ model. The ~~6m~~$6m$ model run from ~~24km~~$24km$ seaward of the CMO site is also a very good match for several of the observed waves. A large fraction of observed waves with amplitude less than ~~15m~~$15m$, and particularly less than ~~10m~~$10m$, are much 'thinner' than model waves with similar amplitudes. However, it seems reasonable to say that the observed waves are a good fit to the model waves.

While some features of the observations are reproduced in the model, there are many differences. The eKdV model used here is highly idealized. There are many effects that have not been ~~included~~considered, including bottom and internal friction, earth's rotation and mean shear. Given these limitations, we conclude that the observations are reasonably well matched by our model.

~~3~~4. Summary and conclusions

Observations of highly nonlinear internal waves contained in the first mode time series on the mid-continental shelf and in current meter records in shallow water have led us to investigate the transformation of the shoaling internal tide. Observations were made in the mid-continental shelf at the site of the Coastal Mixing and Optics Experiment (CMO). An existing model based on generalized KdV and eKdV equations

Formatted: Numbered + Level: 1 + Numbering Style: 1, 2, 3, … + Start at: 3 + Alignment: Left + Aligned at: 0.63 cm + Indent at: 1.27 cm

has been simplified for use in a two-layer ocean, which is representative of realistic stratification. The model accounts for weakly nonlinear and dispersive properties of the internal tide. Earth's rotation, internal dissipation, bottom friction, and internal shear are not included. The internal tide was forced with a periodic sinusoidal boundary condition and allowed to propagate shoreward.

The model was first run within a KdV framework with realistic continental shelf, constant sloping bottom with flat and sloping interface, and CMO shelf parameters. The internal tide steepens on its back face as it propagates shoreward, ~~which is~~ a direct result of the much greater magnitude of the nonlinear term in comparison with the dispersive term. Nonlinear waves evolve from the internal tide after the back face forms a shock-like front. The waves can appear as a rank ordered packet with the leading waves traveling fastest, since they are the most nonlinear. The leading waves of depression usually travel faster than the linear wave speed, c, and nearly fit solitary wave form for local KdV parameters ("sech^2"). ~~The trailing waves usually travel slower than c, tend to be thinner than the local sech^2 waves and are relatively more dispersive than the leading~~Waves of elevation also develop into sech^2 waves.

~~The transformation of the internal tide is dependent upon the ratio of the nonlinear to linear terms, $\alpha\eta/c$, in the KdV equation: for greater values of this ratio the internal tide steepens sooner and nonlinear waves are emitted sooner. The amplitude of the jump and subsequent waves is dependent upon the initial tidal amplitude: larger tidal amplitudes imply larger jump and nonlinear wave amplitudes. For a fixed nonlinear parameter, α, the internal tide becomes nonlinear sooner upon decreasing the value of the dispersive parameter, β.~~

~~The nonlinear waves are waves of depression when the nonlinear parameter, α, is negative, and waves of elevation when it is positive. If a packet of waves of depression propagates into a region where $\alpha > 0$ the~~

~~minima, or troughs, of the waves of depression become maxima, or peaks, of the waves of elevation as they flip polarity.~~

~~All of the~~The model runs made within the KdV framework were also made within the eKdV framework which includes a cubic nonlinearity term scaled by α_1. The results may or may not be similar, depending upon the ratio of the two nonlinear terms, $\frac{\alpha}{\alpha_1 \eta}$. If this ratio is large (much greater than one) the cubic nonlinear term is not important and the KdV and eKdV results are similar. If the ratio is of order one or less the eKdV may evolve differently from the KdV. For ~~most of~~ the constant bottom slope simulations the model results were similar in both frameworks. However, there are some significant differences to the waves that cross the shelf using CMO parameters. The modeled leading waves at the CMO mooring site were much 'thicker' than $sech^2$ waves with local KdV parameters, but they had not quite developed into solitary wave solutions of the eKdV equation ('tanh' or table-top waves).

To better understand the evolution of waves toward ~~tanh~~table-top form in an eKdV framework, without the complications of varying parameters, model runs were made using constant eKdV parameters representative of the CMO site. Upon formation, the leading waves of the packet are similar to $sech^2$ waves. The waves become 'thicker' and tend toward the ~~tanh~~table-top form upon further propagation, but never reach the theoretical tanh curve in our limited domain. To help understand why the evolution of waves from being close to $sech^2$ waves to being close to tanh waves was so slow, the internal tide was forced with a $sech^2$ wave. The evolving $sech^2$ rapidly moves to the theoretical tanh curve for all amplitudes. We conclude that the interaction between the solitary like-waves in a packet slows them from evolving into exact solitary '$sech^2$' or 'tanh' waves.

Formatted: Font: 14 pt

Model runs with varying initial amplitudes and generation regions were made to help interpret the observations made at the CMO site. Some features of the observations compare well with the model. The leading face of the internal tide steepens to form a shock like front. Nonlinear high frequency waves evolve shortly after the appearance of the jump. Although not rank ordered, the wave of maximum amplitude is always close to the jump. Some features of the observations are not found in the model. Nonlinear waves can be very widely spaced and persist over a tidal period. The amplitude of the observed waves often decreases before the arrival of the jump, while the leading face may change slope before the jump arrives.

Individual observed waves were examined and the details compared to model results. The observed nonlinear waves vary greatly in amplitude and width, generally having amplitudes of between 5 and 25 metres, and widths of between 200 and 600 seconds. Larger amplitude waves are well approximated by waves evolving from large amplitude model waves. A large fraction of smaller amplitude observed waves, particularly less than 10 m, are thinner than model waves of similar amplitude. We conclude that the observed waves are a good match to modeled waves given the highly idealized eKdV model used, and the fact that we have neglected friction, rotation and mean shear.

Author Contribution

Kieran O'Driscoll conducted this work out while a graduate student at the College of Oceanic & Atmospheric Sciences, Oregon State University, in partial fulfillment of the degree of Master of Science. Murray Levine was the student's advisor.

Acknowledgements

Kieran O'Driscoll would like to thank Jack Barth for a considerable review of a previous version of this manuscript., and two referees for considerable reviews and helpful comments. This work was supported by funding from the Office of Naval Research and Oregon State University.

Competing interests: Kieran O'Driscoll declares that he has no conflict of interest.

References

Alford, M.H. and Zhao, Z.: Global patterns of low-mode internal-wave propagation. Part I: Energy and energy flux. J. Phys. Oc., 37, 1829-1848, 2007.

Apel, J.R.: Principles of ocean physics, International Geophysics Series, Volume 38, Academic Press, pp. 634, 1987.

Apel J.R., R.F. Gasparovic, D.R. and Thompson, B.L. Gotwols.: Signatures of surface wave/internal wave interactions: Experiment and theory." Dyns. Atms. Ocs., 12, 89-106, 1988.

Barth, J. A., Bogucki, D., Pierce, S. D., and Kosro, P. M.: Secondary circulation associated with a shelfbreak front. Geophys.l Res. Letts., 25, 2761-2764, 1988.

Benney, D.J.: Long nonlinear waves in fluid flows. J. Math. Phys., 45, 52 – 63, 1966.

~~Berezin Yu.A.: Modeling Nonlinear Wave Processes. VNU Science Press, pp. 182, 1987.~~

Boyd, T., Levine, M.D., and Gard, S.R.: Mooring observations from the Mid-Atlantic Bight, Oregon State University, Data Report 97-2, pp. 226, 1997.

Cacchione, D.A. and Drake, D.A.: Nepheloid layers and internal waves over continental shelves and slopes, Geo-Marine Lett., 6, 147-152, 1986.

Formatted: Font: +Body (Times New Roman)

Formatted: Font: +Body (Times New Roman)

~~Drazin, P.G. and Johnson, R.S.: Solitons: an introduction, Cambridge texts in applied mathematics, Cambridge University Press, pp. 226, 1989.~~

Cushman-Roisin, B. and Beckers, J-M.: Introduction to geophysical fluid dynamics: physical and numerical aspects. Vol. 101. Academic Press, 2011.

Garrett, C. and Munk, W.: Internal waves in the ocean, Ann. Rev. Fluid Mech., 11, 339-369, 1979.

Gill, A.E.: Atmosphere-Ocean Dynamics, Academic Press, Inc., pp.662, 1982.

Grimshaw, R.: Slowly varying solitary waves. I. Korteweg - de Vries equation. Proc. R. Soc., Lond., Ser. A, 368, 359-375, 1979.

Grimshaw, R., Pelinovsky, D., Pelinovsky, E., and Slunyaev, A.: Generation of large-amplitude solitons in the extended Korteweg–de Vries equation. Chaos: An Interdisciplinary Journal of Nonlinear Science, 12, 1070-1076, 2002.

Grimshaw, R., Pelinovsky, E., Talipova, T., and Kurkin, A.: Simulation of the transformation of internal solitary waves on oceanic shelves. J. Phys. Oc., 34, 2774-2791, 2004.

Grimshaw, R., Pelinovsky, E., Talipova, T., and Kurkina, O.: Internal solitary waves: propagation, deformation and disintegration~~.~~, Nonlinear Processes in Geophysics, 17, 633-649, 2010.

Grimshaw, R., Guo, C., Helfrich, K. and Vlasenko, V.: Combined effect of rotation and topography on shoaling oceanic internal solitary waves, J. Phys. Oc., 44, 1116-1132, 2014.

Holloway, P.E.: On the semidiurnal internal tide at a shelf-break region on the Australian North-West Shelf, J. Phys. Oc., 14, 1787-1799, 1984.

Holloway, P.E.: Internal hydraulic jumps and solitons at a shelf break region on the Australian North West Shelf. J. Geophys. Res. Oc., 92, 5405-5416, 1987.

Holloway, P.E., Humphries, S.E., Atkinson, M., and Imberger, J.: Mechanisms for nitrogen supply to the Australian North-West Shelf. Aust. J. Mar. Freshw. Res., 36, 753-764, 1985.

Holloway, P.E., Pelinovsky, E., Talipova, T., and Barnes, B.: A nonlinear model of internal tide transformation on the Australian North West Shelf. J. Phys. Oc., 27, 871-896, 1997.

Lamb, K.G. and Yan, L.: The evolution of internal wave undular bores: Comparisons of a fully nonlinear numerical model with weakly-nonlinear theory, J. Phys. Oc., 26, 2712 – 2734, 1996.

Formatted: Font color: Custom Color(RGB(34,34,34)), Pattern: Clear (White)

Formatted: Font color: Custom Color(RGB(34,34,34)), Pattern: Clear (White)

Formatted: Font: +Body (Times New Roman)

~~Lapidus, L. and Pinder, G.F.: Numerical solution of partial differential equations in science and engineering, John Wiley & Sons, Inc., pp. 677, 1982.~~

Lamb, K. G. and Warn-Varnas, A.: Two-dimensional numerical simulations of shoaling internal solitary waves at the ASIAEX site in the South China Sea, Nonlinear Processes in Geophysics, 22, 289-312, 2015.

Lamb, K.G. and Xiao, W.: Internal solitary waves shoaling onto a shelf: Comparisons of weakly-nonlinear and fully nonlinear models for hyperbolic-tangent stratifications, Ocean Model, 78, 17-34, 2014.

Lee, C. and Beardsley, R.C.: The generation of long nonlinear internal waves in a weakly stratified shear flow, J. Geophys. Res., 79, 453-462, 1974.

Levine, M. and Boyd, T.: Nonlinear internal wave observations on the continental shelf. In The 1998 WHOI/IOS/ONR Internal Solitary Wave Workshop: Contributed Papers, 1999.

Lighthill, J.: Waves in fluids, Cambridge University Press, pp. 504, 1978.

Munk, W.H.: Internal waves and small-scale processes. Evolution of Physical Oceanography (B.A. Warren & C. Wunsch, eds.), Chapter 9. MIT press, Cambridge Massachusetts, 1981.

O'Driscoll, K.T.A.: Nonlinear internal waves on the continental shelf. MS Thesis, College Oceanic and Atmospheric Sciences, Oregon State Univ., pp.125, 1999.

Osborne, A.R., Burch, T.L., and Scarlet, R.I.: The influence of internal waves on deep-water drilling. J. Pet. Technol., 30, 1497, 1978.

Ostrovsky, L. A. and Stepanyants, Y.A.: Do internal solitons exist in the ocean? Rev. Geophys., 27, 293 310, 1989.

Pelinovsky, E. and Shavratsky, S. Propagation of nonlinear internal waves in the inhomogeneous ocean, Izv. Atmos. Oceanic. Phys., 12, 41 – 44, 1976.

Pelinovsky, E., Shavratsky, S., and Raevsky, M.A.: The Korteweg de Vries equation for nonstationary internal waves in an inhomogeneous ocean, Izv. Atmos. Oceanic. Phys., 13, 373 – 276, 1977.

Sandstrom, H. and Elliott, J.A.: Internal tide and solitons on the Scotian shelf: a nutrient pump at work., J. Geophys. Res., 89, 6415-6426, 1984.

Shea, R.E., and Broenkow, W.W.: The role of internal tides in the nutrient enrichment of Monterey Bay, California, Estuarine, Coastal and Shelf Sci., 15, 57-66, 1982.

~~Stanton, T. P. and Ostrovsky, L.A.: Observations of highly nonlinear internal solitons over the Continental Shelf, Geophys. Res. Letts., 25, 2695-2698, 1988.~~

Willmott, A. and Edwards, P.D.: A numerical model for the generation of tidally forced nonlinear internal waves over topography, Cont. Shelf Res., 7, 457-484, 1987.

(a)

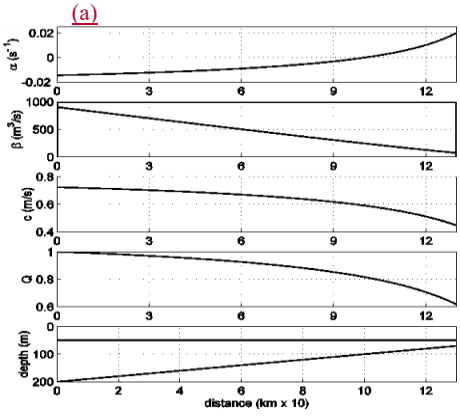

(b)

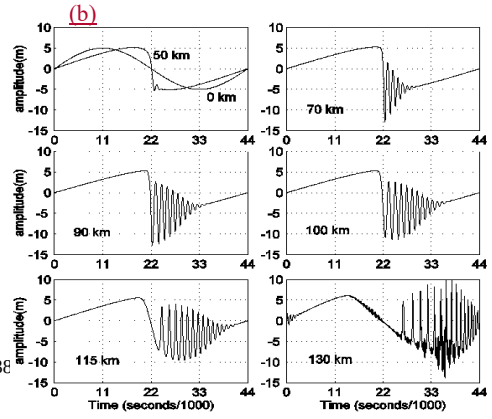

(c)

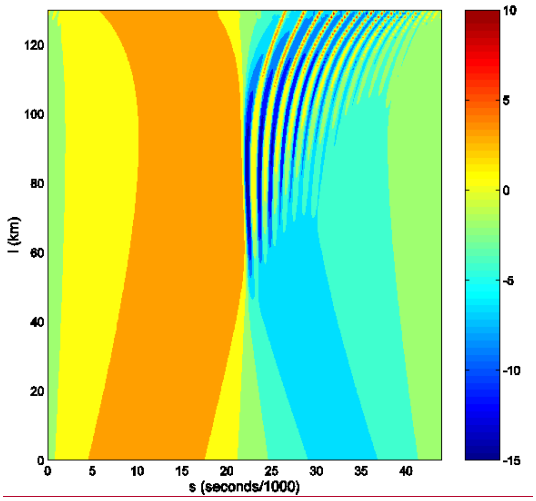

Fig. ~~Zabusky, N.J. and Kruskal, M.D.: Interactions of 'solitons' in a collisionless plasma and the recurrence of initial states~~1. Case A (constant sloping bottom ~~Phys. Rev. Lett., 15, 240-243, 1965.~~

~~Zhou, X. and Grimshaw, R.: The effects of variable currents on internal solitary waves, Dyn. Atm. Oc., 14, 17-39, 1989.~~

Formatted: Font: 12 pt

Formatted: Font color: Custom Color(RGB(34,34,34)), Pattern: Clear (White)

Formatted: Font color: Custom Color(RGB(34,34,34)), Pattern: Clear (White)

~~Figures~~

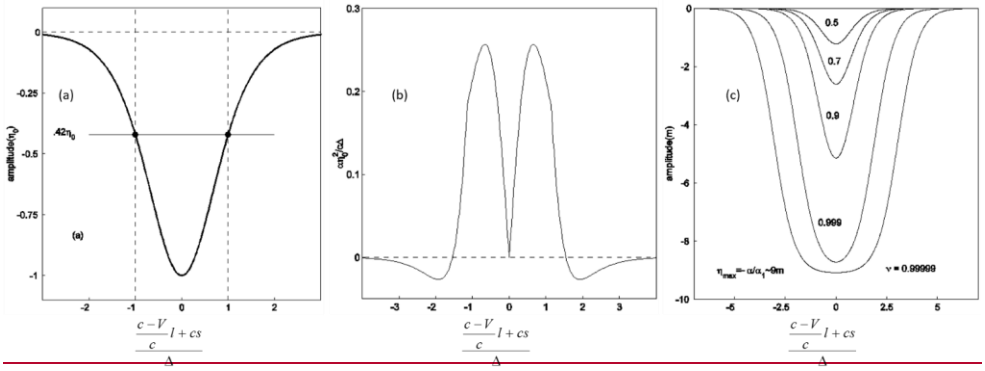

~~Fig1. **(a)** KdV 'sech²' wave~~ with ~~amplitude of -1 m, where the wave argument value is shown on the abscissa and~~ level interface, h_1 = 50 m). KdV parameter values ~~are calculated from Case 1 model runs~~

~~(h_1 = 50 m, h_2 = 150 m, $g\Delta\rho/\rho$ = .014 m/s^2). The amplitude of these waves is reduced to 42% of its maximum value when the argument is 1.~~ **~~(b)~~** ~~The difference of the absolute values of the nonlinear and dispersive terms, χ, in the KdV equation~~ for ~~the 'sech^2' wave shown in (a).~~ **~~(c)~~** ~~eKdV 'tanh' wave for several values of the nonlinear parameter, ν. Parameter values as in (a).~~

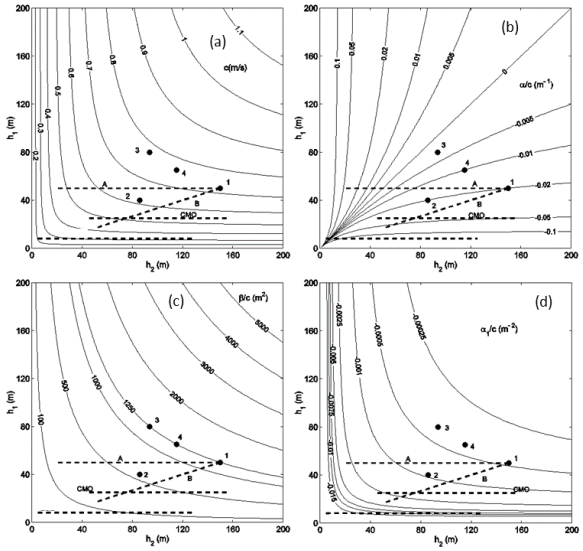

~~Fig. 2. **(a)** Linear wave speed, c(m/s), as a function of the depth of the upper layer, h_1, and lower layer, h_2. Also shown are the values for level bottom (Cases 1-4), sloping bottom (Cases A and B) and realistic slope and stratification (CMO).~~ **~~(b)~~** ~~KdV~~ quadratic nonlinear parameter, α, ~~divided by the linear wave speed, c, as in (a).~~ **~~(c)~~** ~~KdV~~ dispersion parameter, β, ~~divided by the~~ linear ~~wave~~phase speed, c, ~~as in~~horizontal variability factor, Q, and depth **(a)**. ~~**(d)** eKdV cubic nonlinear parameter, α_1, divided by the linear wave speed, c, as in (a).~~

Formatted: Font: Bold

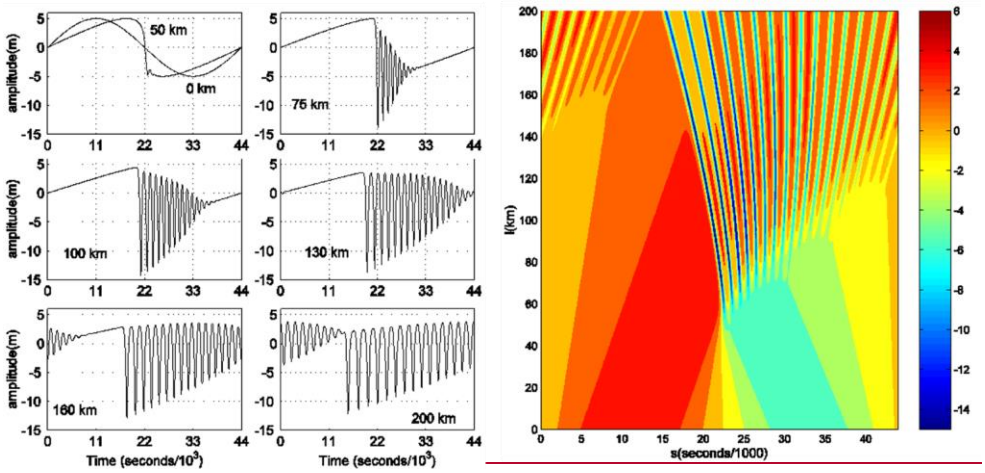

~~Fig. 3. Case 1 (h_1 = 50 m, h_2 = 150 m, level bottom) amplitude~~Amplitude of the internal mode for two-layer fluid **(~~a~~b)** at various distances from the boundary within KdV model framework and **(~~b~~c)** as a function of distance *l* and time *s* within KdV model framework. The legend on the right corresponds to the amplitude of the waves (m).

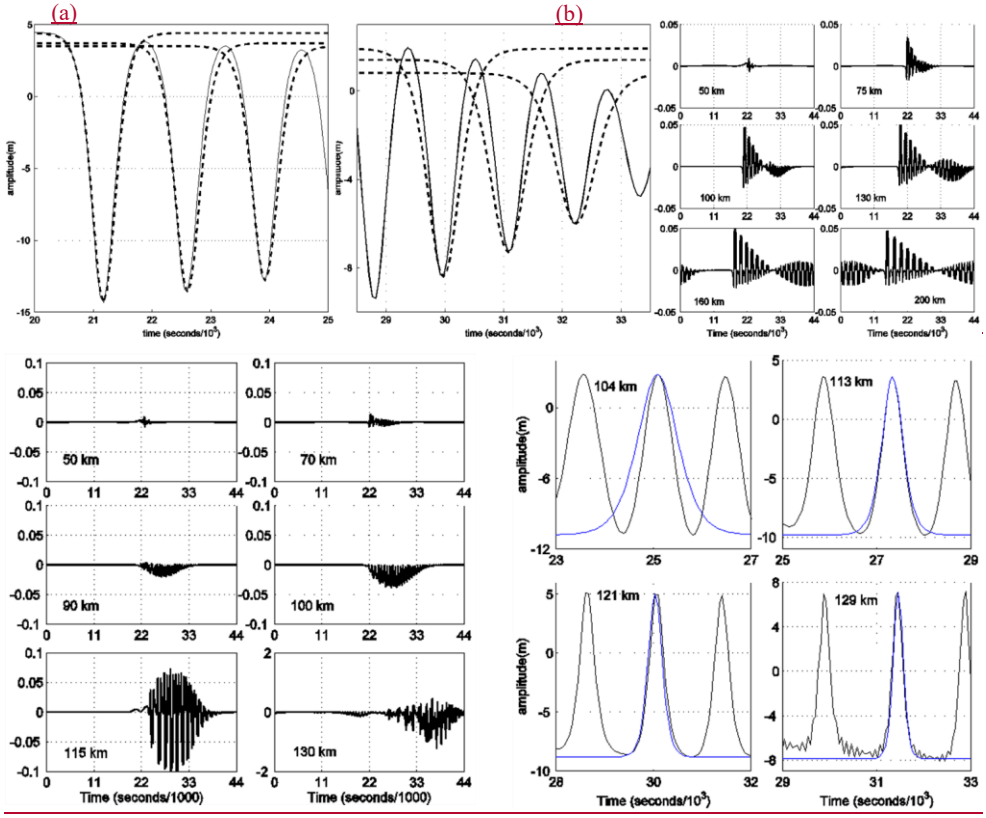

Fig. ~~4. Case 1. **(a)** The three leading waves of depression (solid line) at a distance of 100 km from the boundary shown in Fig. 3a are plotted with three individual sech^2 waves (broken lines).~~

~~**(b)** Same as (a) but for trailing waves in the packet. **(c)** Difference~~2. Case A, **(a)** difference between the magnitudes of the nonlinear and dispersive terms~~, χ (non-dimensional)~~ at various distances from the boundary, and **(b)** leading waves of elevation (black line) at various distances $l > 100km$ from the boundary plotted with individual sech^2 waves (blue lines) within KdV model framework.

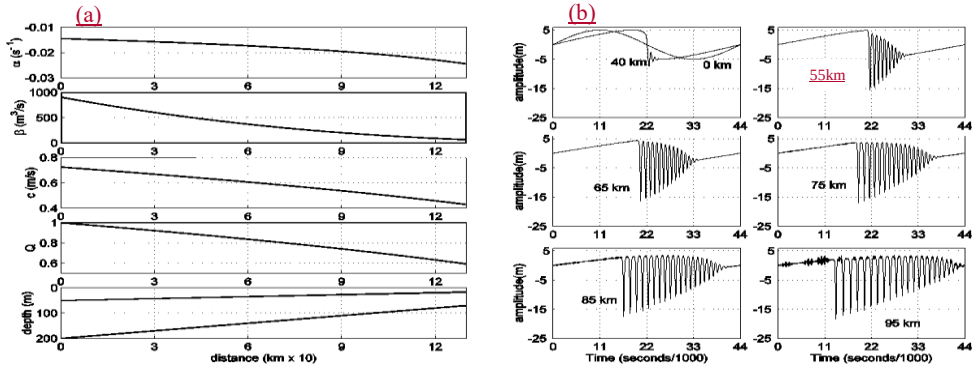
(a)
(b)
α (s⁻¹)
β (m²/s)
c (m/s)
Q
depth (m)
distance (km x 10)
amplitude(m)
40 km
0 km
55km
65 km
76 km
85 km
95 km
Time (seconds/1000)

(c)

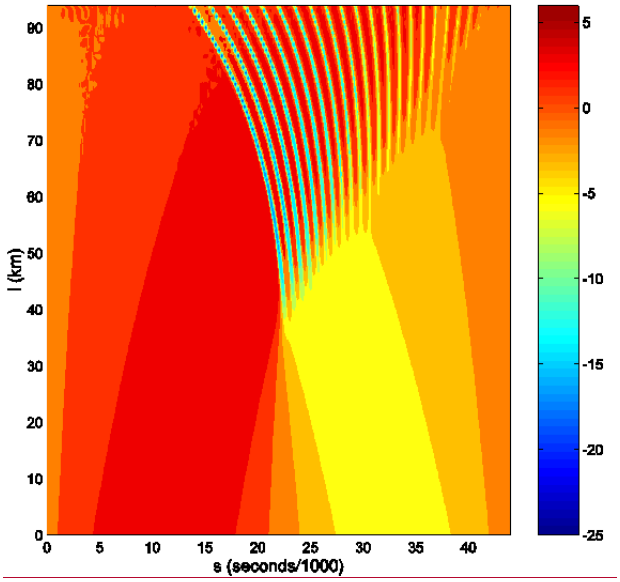
l (km)
s (seconds/1000)
0
10
20
30
40
50
60
70
80
90
0
5
10
15
20
25
30
35
40
5
0
-5
-10
-15
-20
-25

Fig.

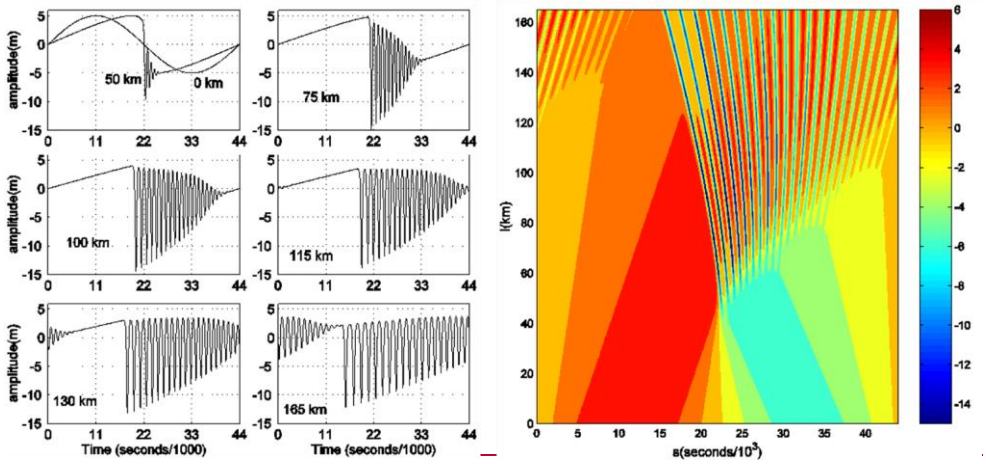

3. Same as Fig. ~~5.~~1 ~~Same as Fig. 3~~ but for Case ~~2 (h_1 = 40 m, h_2 = 85.7 m, level bottom).~~

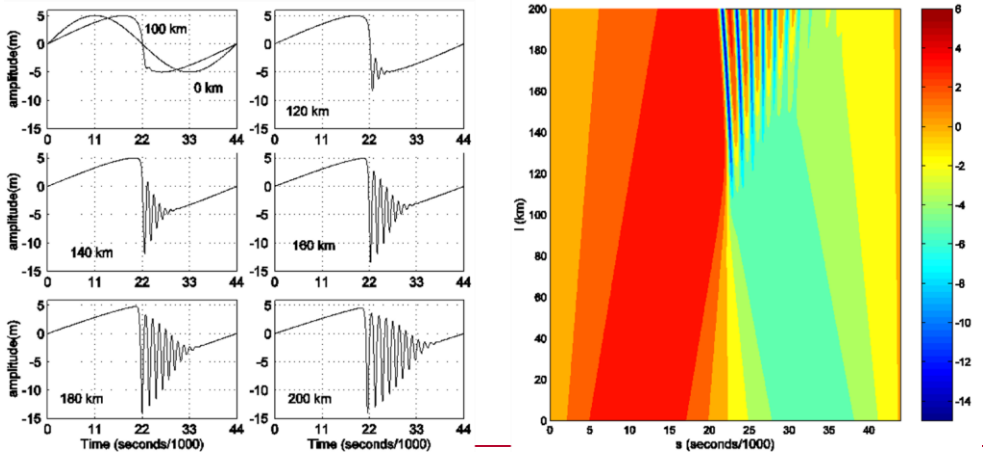

~~Fig. 6. Same as Fig. 3 but for Case 4 (h_1 = 65.1 m, h_2 = 115.1 m, level bottom.~~

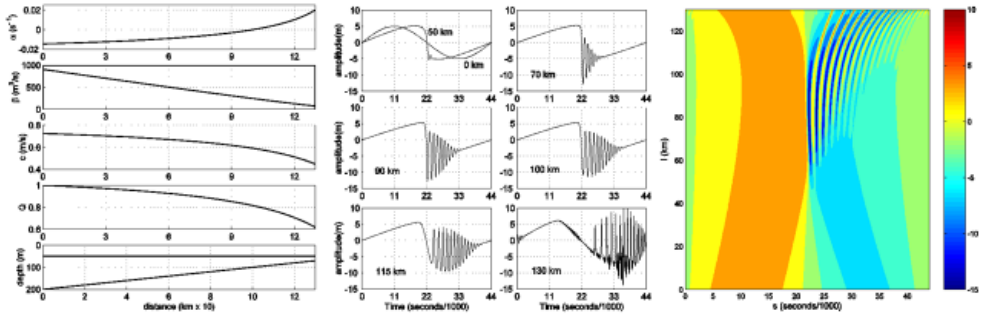

~~Fig. 7. Case A~~B (constant sloping bottom with ~~level~~sloping interface~~, h_1 = 50 m~~). ~~**(a, left)** KdV parameter values for quadratic nonlinear parameter, α, dispersion parameter, β, linear phase speed, c, horizontal variability factor, Q, and depth. **(b, center)** and **(c, right)** Same as Fig. 3 but for Case A parameters.~~).

(a)

(b)

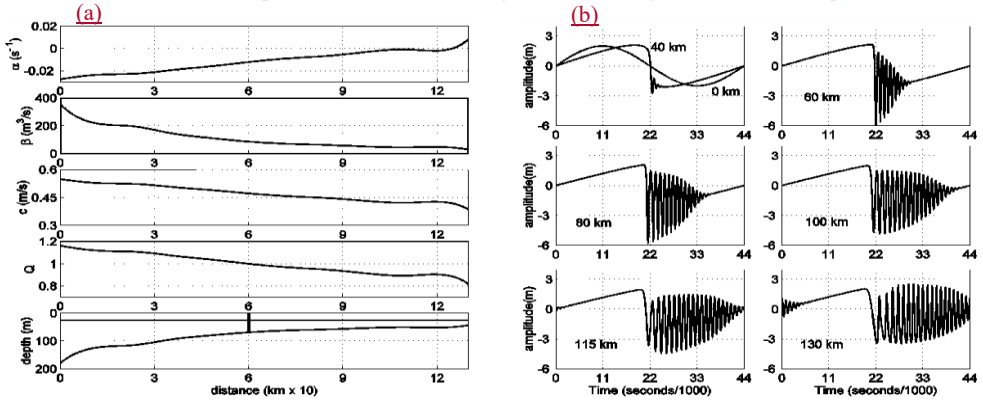

(c)

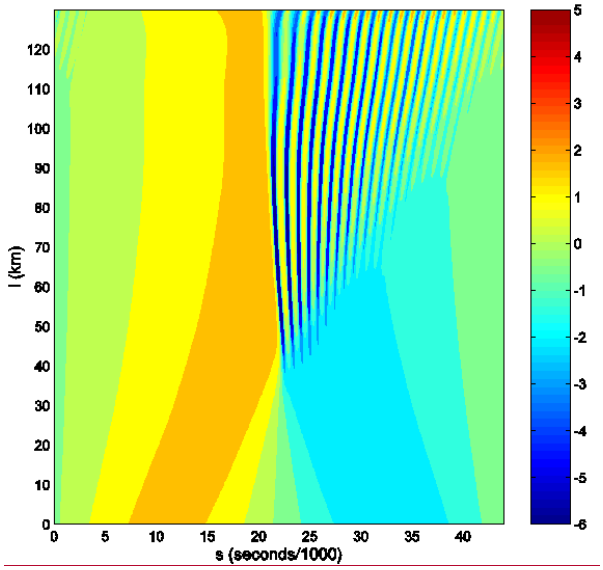

Fig. 4. Same as Fig.

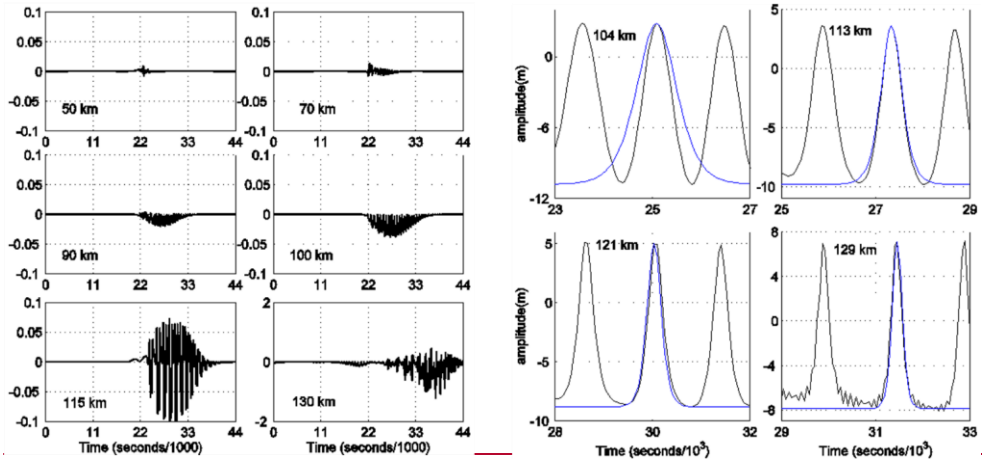

~~Fig. 8. Case A, **(a, left**~~1 but for CMO experiment site (with flat interface, $h_1 = 25\ m$).

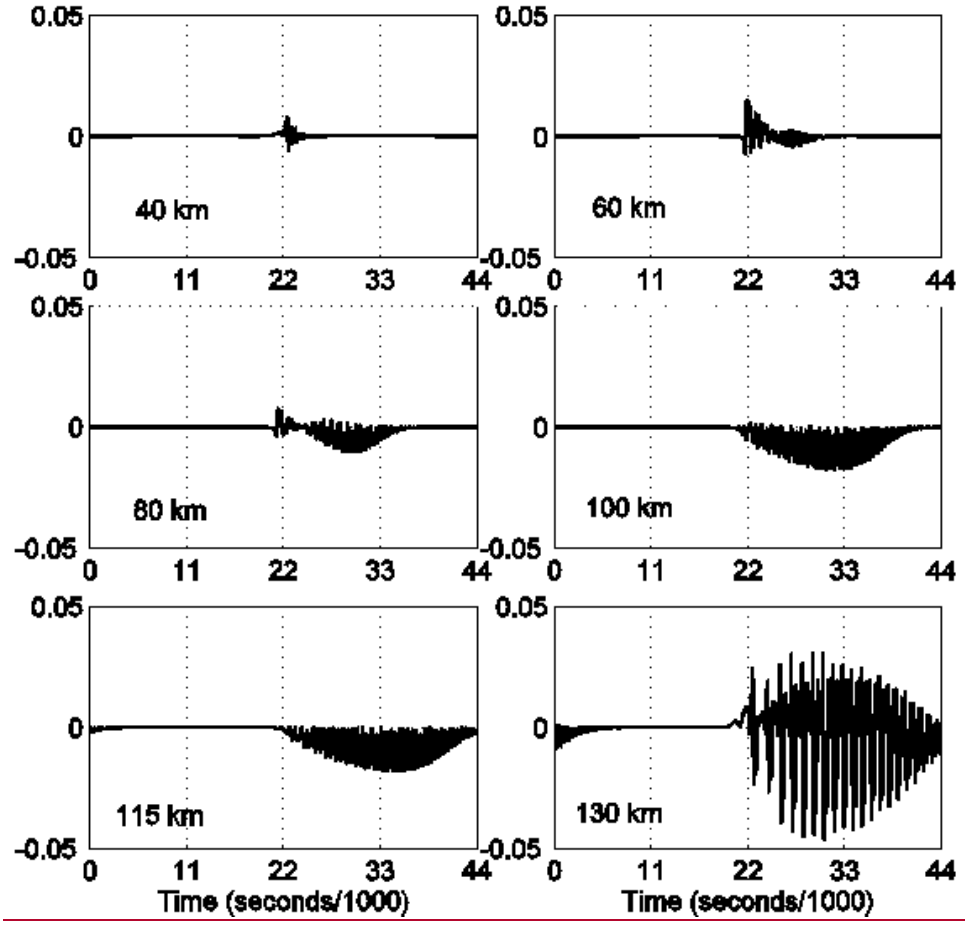

Fig. 5. CMO experiment site (with flat interface, $h_1 = 25\ m$) difference between the magnitudes of the nonlinear and dispersive terms at various distances from the boundary~~, and **(b, right)** leading waves of elevation (black line) at various distances greater than 100km from the boundary plotted with individual $sech^2$ waves (blue lines)~~ within KdV model framework.

Formatted: Font: Not Bold

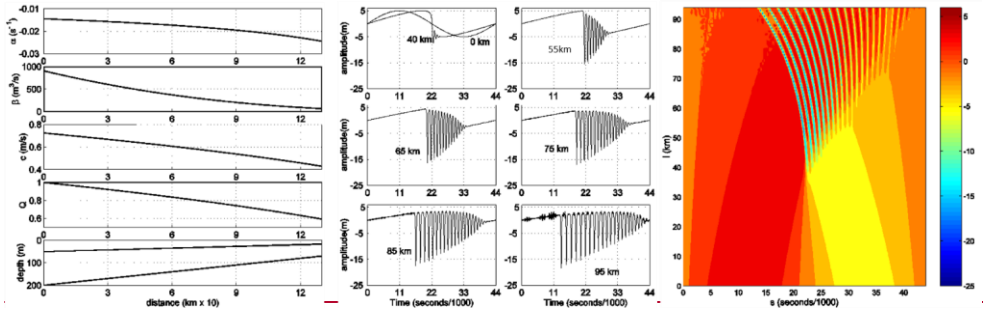
distance (km x 10)
Time (seconds/1000)
Time (seconds/1000)
s (seconds/1000)
l (km)
40 km
0 km
55km
65 km
75 km
85 km
95 km

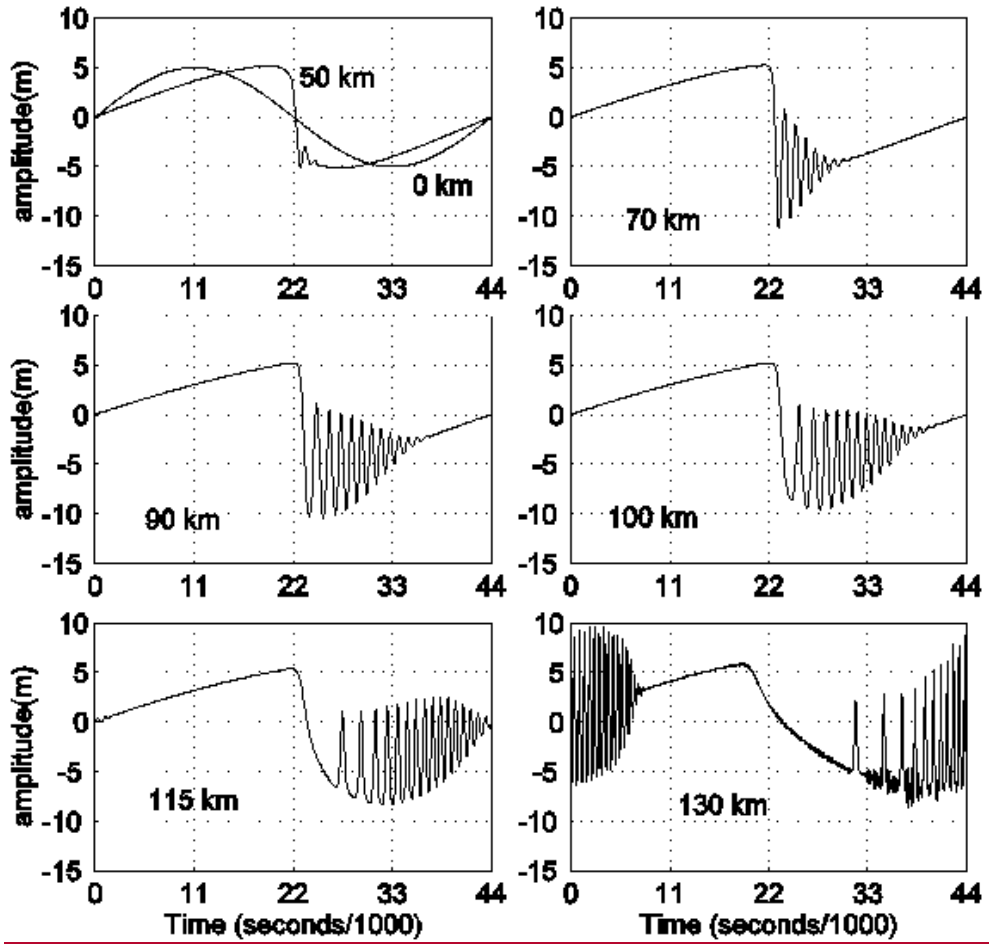

Fig. ~~9. Same as Fig. 7 but for Case B (constant sloping bottom with sloping interface).~~

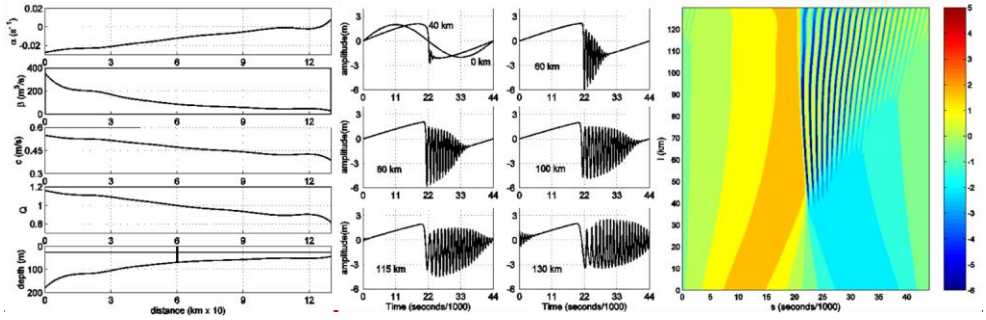

~~Fig. 10. Same as Fig. 7 but for CMO experiment site (with flat interface, h_1 = 25 m).~~

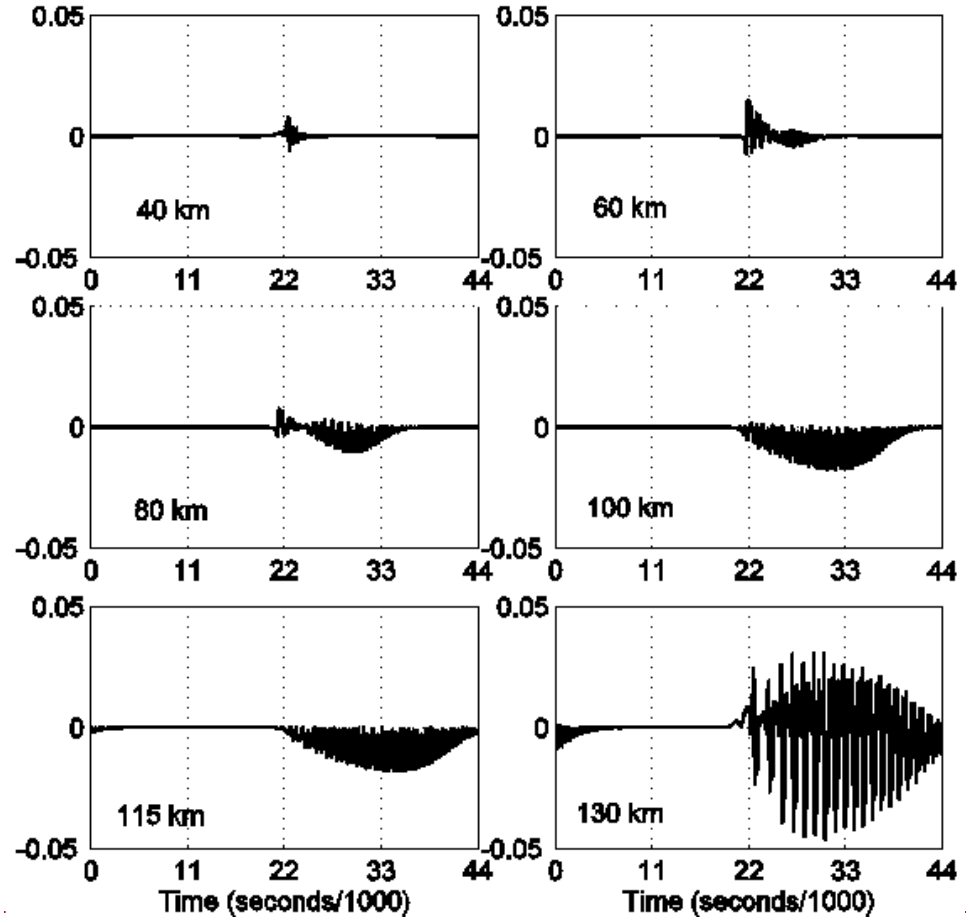

Fig. 11. CMO experiment site (with flat interface, $h_1 = 25$ m) difference between the magnitudes of the nonlinear and dispersive terms at various distances from the boundary within KdV model framework.

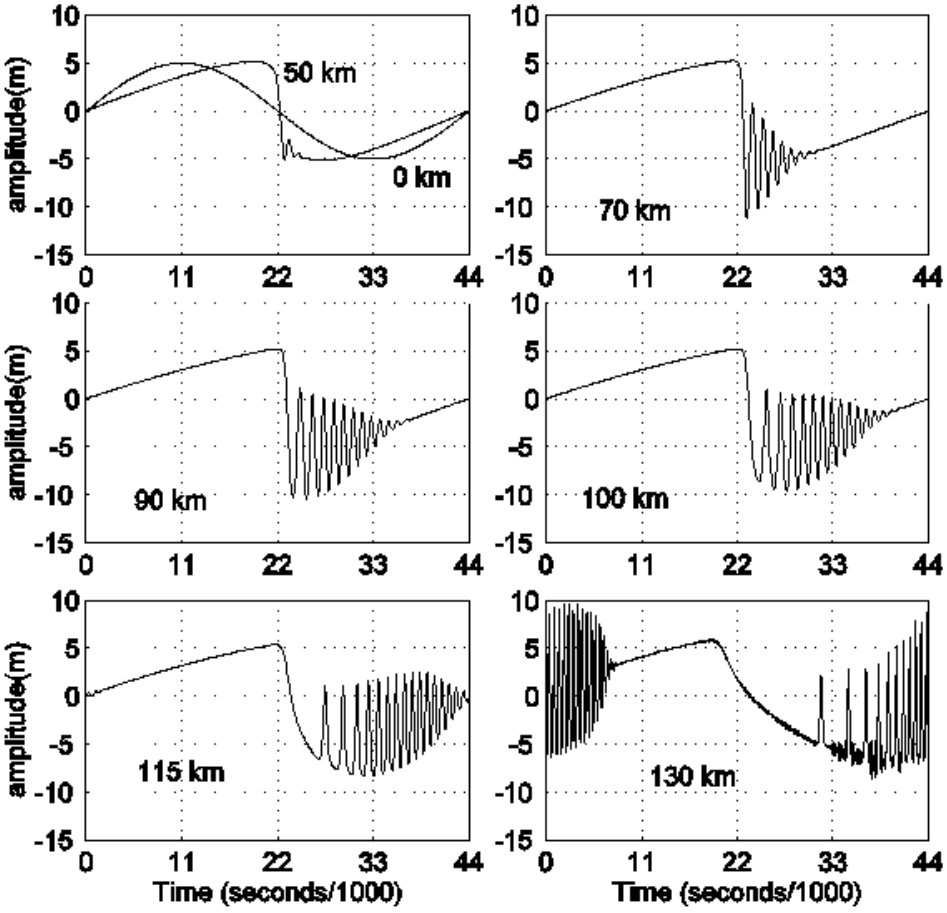

~~Fig. 12~~6. Case A (constant sloping bottom with flat interface, ~~$h_1 = 50$ m~~$h_1 = 50\ m$) amplitude of the internal mode for two-layer fluid at various distances from the boundary within eKdV model framework.

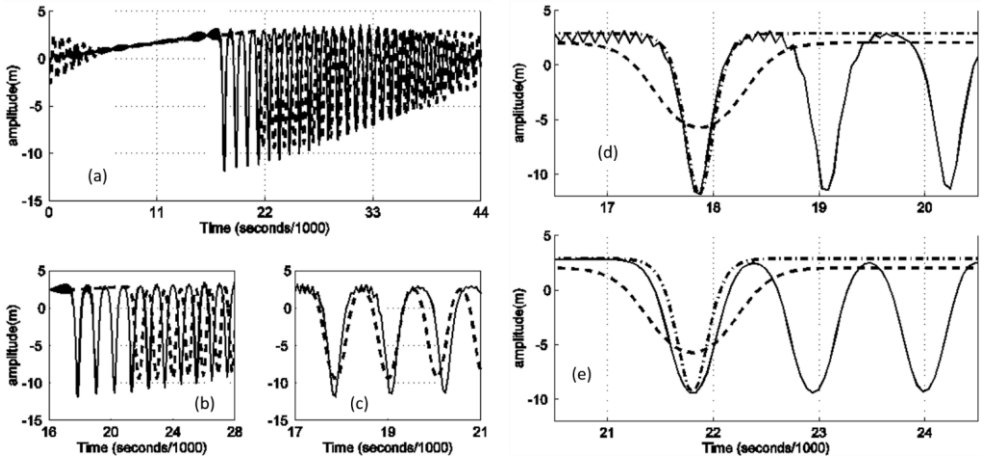

Fig. ~~13~~7. CMO experiment site (realistic topography with level interface, ~~$h_1 = 25$ m~~($h_1 = 25\,m$) amplitude of the internal mode for two-layer fluid at ~~60 km~~$60\ km$ in ~~69 m~~$69\ m$ depth water (CMO mooring site). **(a)** Comparison of KdV (solid line) and eKdV (broken line) solutions. **(b)** Close up of (a). **(c)** Leading KdV model waves (solid line) with superimposed eKdV model waves (broken line) shifted forward in time (s) so that the leading waves coincide. **(d)** and **(e).** The leading wave of depression (solid line) plotted with an individual sech^2 wave (dot-dash line) and with an individual tanh wave (dashed line) for KdV model (d), and eKdV model (e).

Formatted: Centered

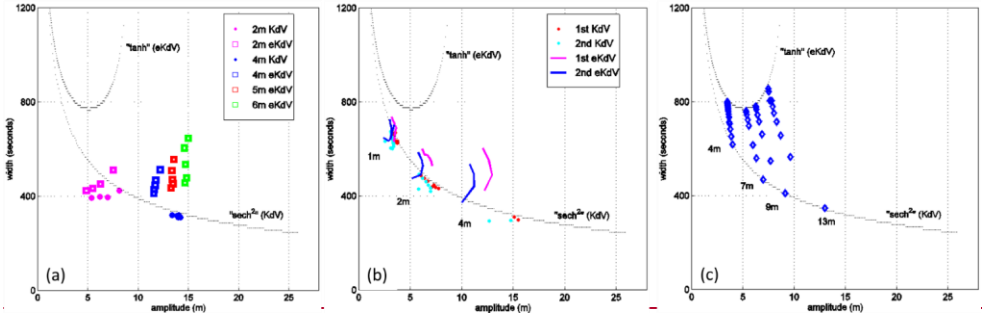

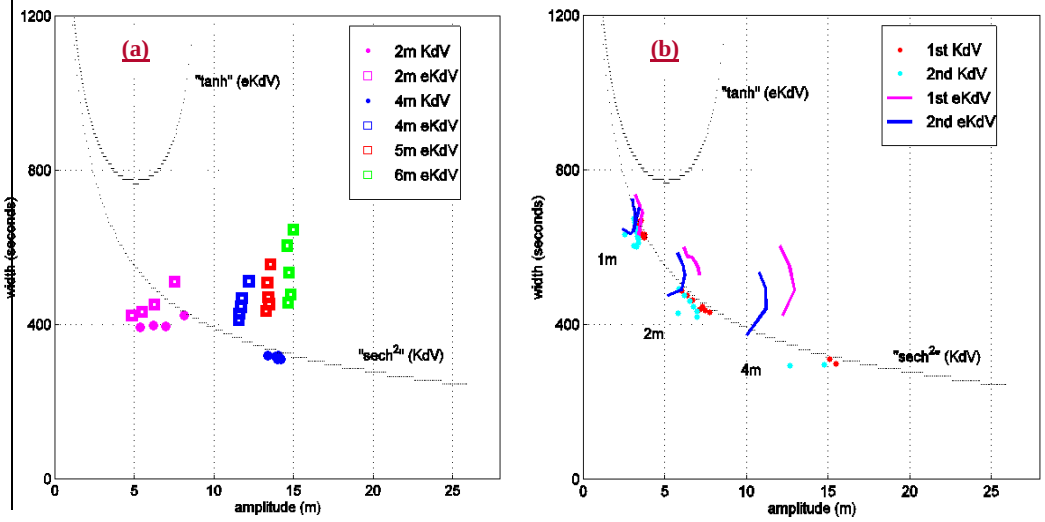
(a)
"tanh" (eKdV)
"sech²" (KdV)
2m KdV
2m eKdV
4m KdV
4m eKdV
5m eKdV
6m eKdV
width (seconds)
amplitude (m)
0
400
800
1200
0
5
10
15
20
25

(b)
"tanh" (eKdV)
"sech²" (KdV)
1st KdV
2nd KdV
1st eKdV
2nd eKdV
1m
2m
4m
width (seconds)
amplitude (m)
0
400
800
1200
0
5
10
15
20
25

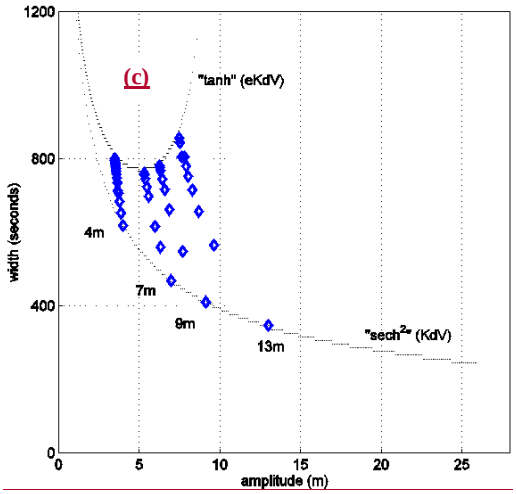

Fig. ~~14 (a)~~8 Width vs. amplitude of the leading waves of the KdV and eKdV solutions at the CMO mooring site (~~h_1 = 25 m, h_2 = 44m~~$h_1 = 25\ m, h_2 = 44m$) at ~~60 km~~$60\ km$ from the boundary in ~~69 m~~$69\ m$ depth water. Results for initial tidal amplitudes of 2, 4, 5, and 6 m are shown. The theoretical values for sech^2 and tanh waves using local parameters are also shown (dotted lines). The width is calculated at 42% of the total amplitude. **(b)** Evolution of the width vs. amplitude of the two leading waves of the KdV and eKdV solutions for flat bottom (h_1 = 25 m, h_2 = 44 m) with same parameters as at the CMO site. Results for initial tidal amplitudes of 1, 2, and 4 m are shown. A value is plotted every 10 km for the 1 m tide beginning at 160 km and the lines run from 160 km to 260 km. A value is plotted every 20 km for the 2 m tide beginning at 80 km and the lines run from 80 km to 200 km. A value is plotted every 20 km for the 4 m tide beginning at 40 km and the lines run from 40 km to 100 km. The theoretical width vs. amplitude for sech^2 and tanh waves is also shown (dotted lines), and the width is calculated at 42% of the total amplitude. **(c)** Evolution of the width vs. amplitude of four solitary sech^2 waves of the eKdV solutions for flat bottom (h_1 = 25 m, h_2 = 44 m) with same parameters as at the CMO site. Results are shown for sech^2 amplitudes of 4, 7, 9 and 13 m. A value is plotted every 1 km up to a

maximum distance of 15 km. The theoretical width vs. amplitude for $sech^2$ and tanh waves is also shown (dotted lines). The width is calculated at 42% of the total amplitude.

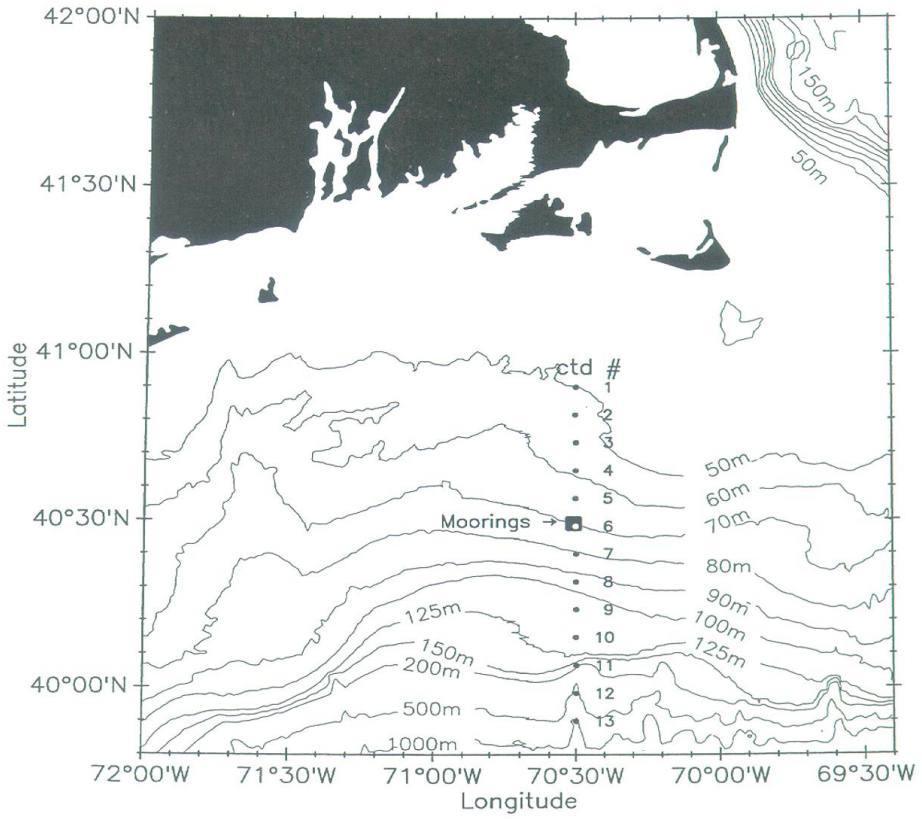

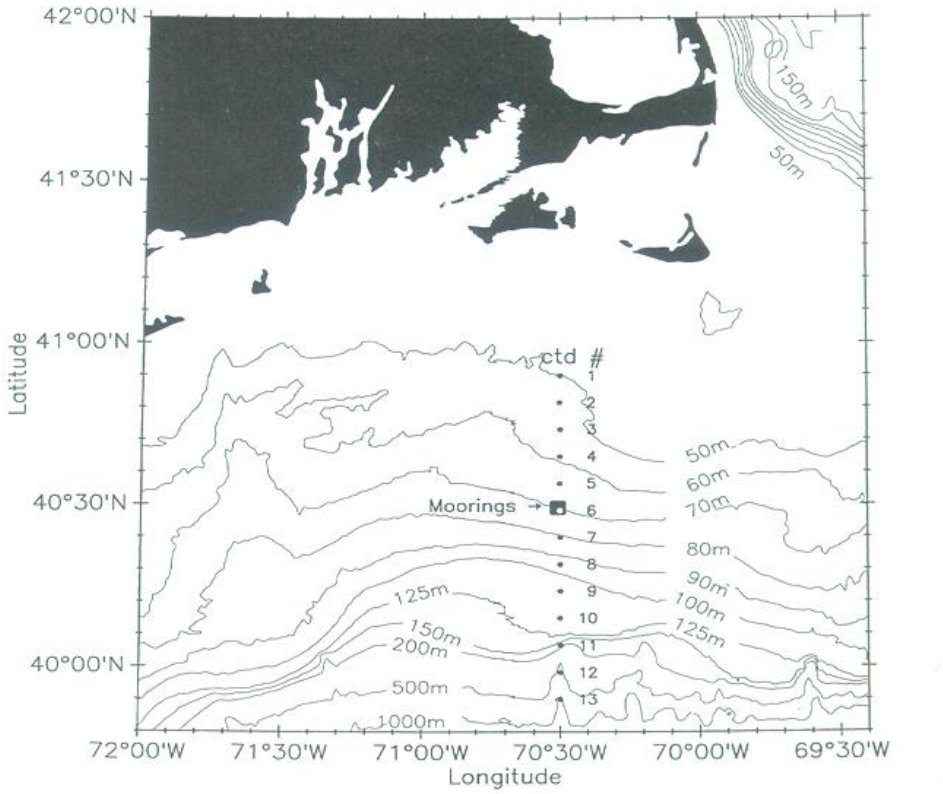

Fig. ~~15~~9. Site of the Coastal Mixing & Optics experiment (left) located in the Middle Atlantic Bight to the south of Massachusetts. The data discussed was collected at the mooring marked 'CTD #6'.

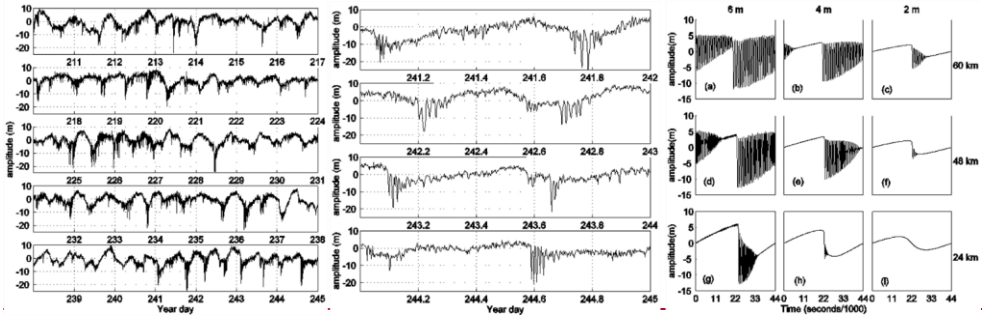
6 m
4 m
2 m
60 km
48 km
24 km
amplitude (m)
Year day
Time (seconds/1000)

i)

ii)

iii)

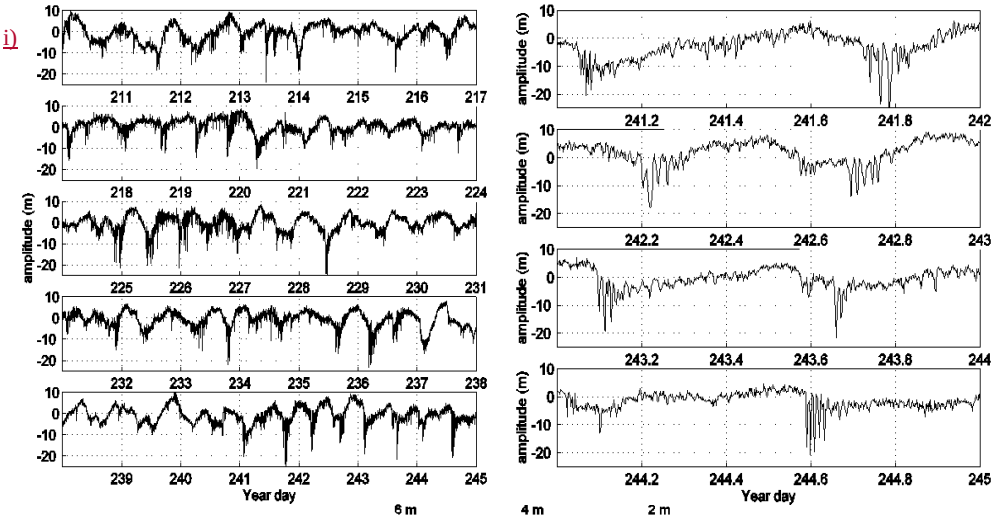
amplitude (m)
Year day

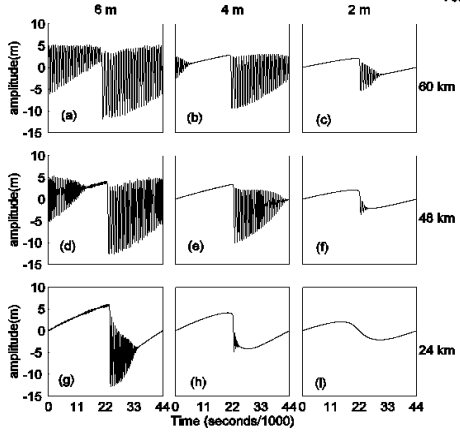
6 m
4 m
2 m
60 km
48 km
24 km
amplitude(m)
Time (seconds/1000)

Fig. ~~16. (a) Left panel: Amplitude~~10. Top left, i), amplitude of the first internal mode calculated from the current meter record at the CMO mooring site over the period day 210-245 of 1996. ~~(b) Center panel:~~Top right, ii), Same as ~~left panel~~i) except for the period day 241-245. ~~(c) Right panel: Three~~Bottom, iii), three sinusoids of amplitude 2 m, 4 m and 6 m, respectively, and with tidal period, as they appear at the CMO mooring site in the eKdV framework. ~~-~~The sinusoids have propagated shoreward from boundaries at 60 km, 48 km and 24 km offshore, respectively.

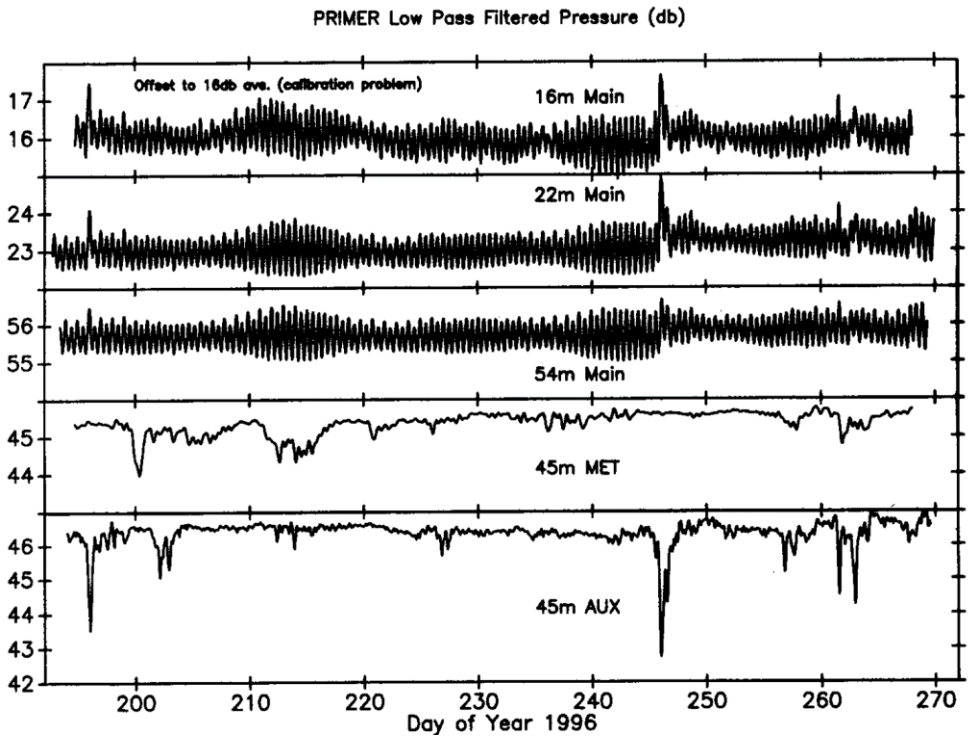

Fig. ~~17~~11. Pressure (tidal) record at the CMO mooring site ~~(top) over~~including for the period day 210 – 245 1996 (from Boyd et al., 1997).

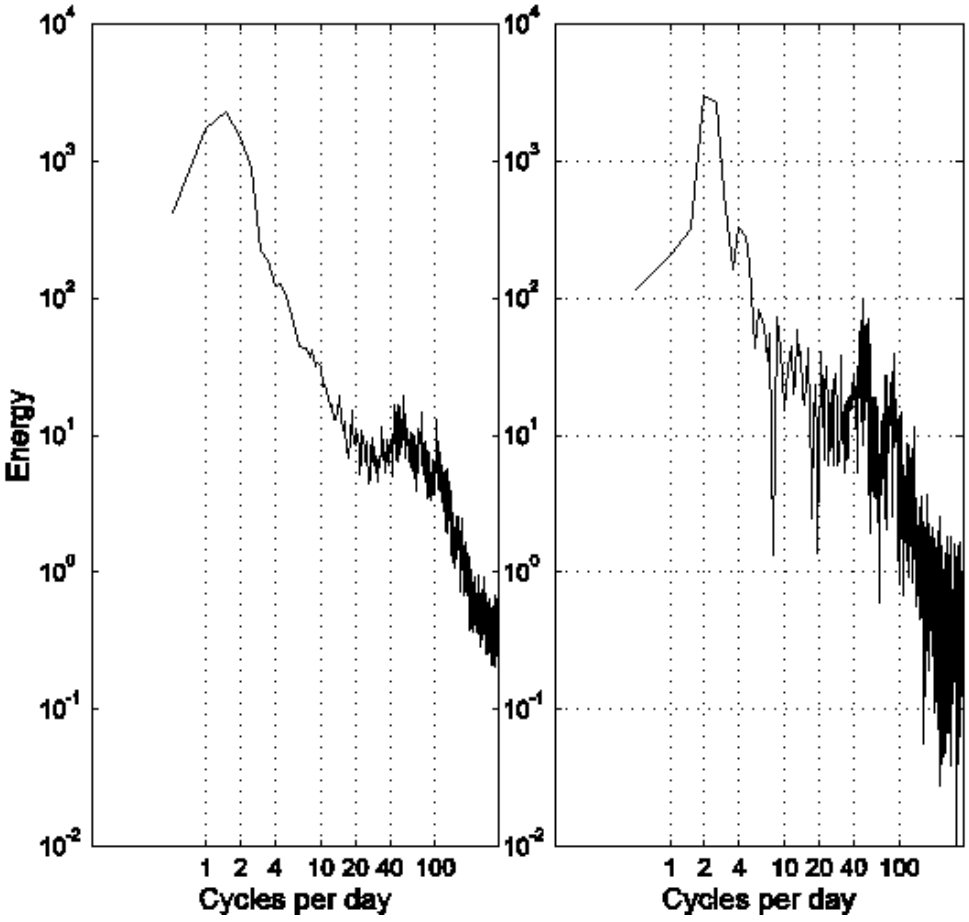

Fig. ~~18~~12. Energy spectra of the first internal mode at the CMO mooring for the period day 210 – 245 (left), and the period 241 – 245 (right).

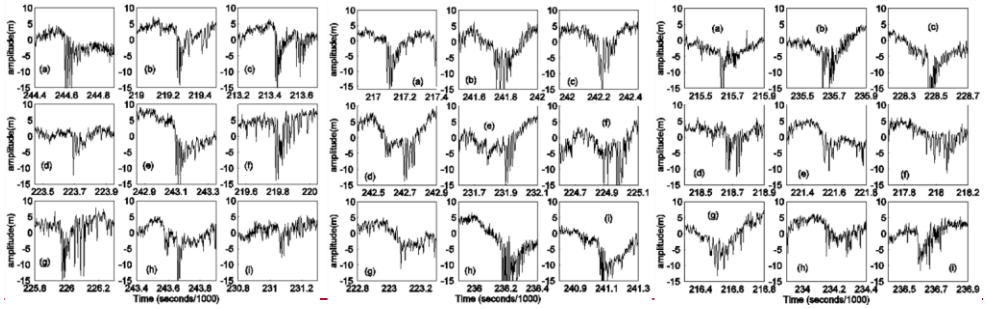

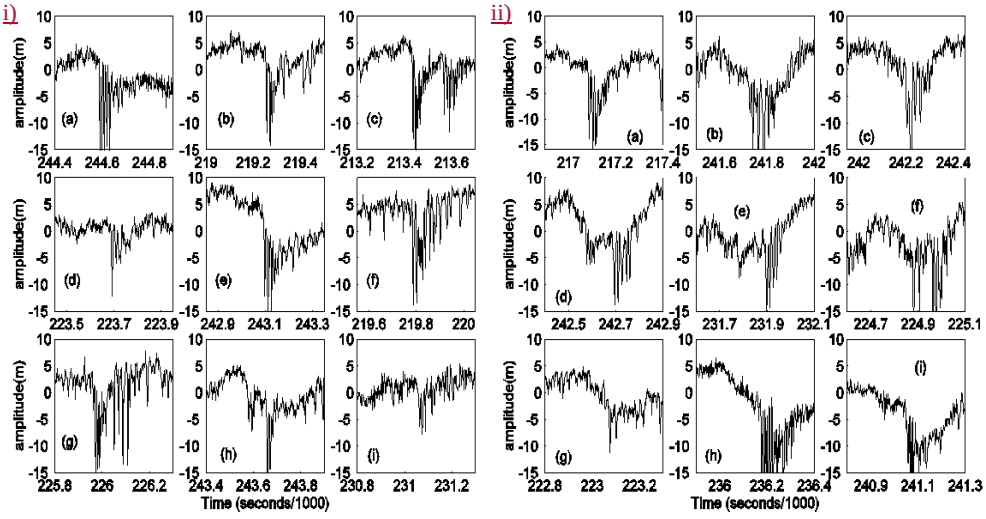
i)
ii)
amplitude(m)
(a)
(b)
(c)
(d)
(e)
(f)
(g)
(h)
(i)
Time (seconds/1000)

iii)

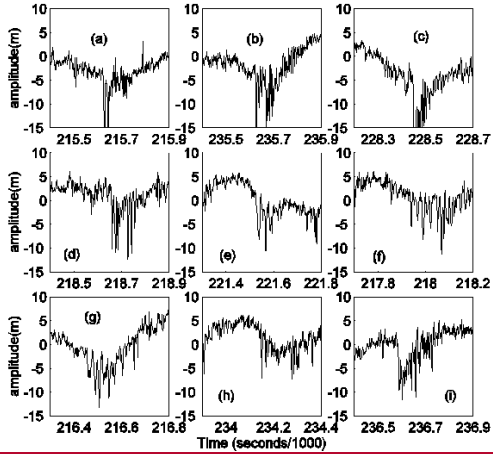

Fig. ~~19~~13. Observations at the CMO Mooring site over a semi-diurnal period. ~~**Left:** These~~Top left, i), sections of the record ~~were chosen since they are~~ similar to events observed over a tidal period in the model runs of Fig. ~~16c. **Center:** Same~~10 iii). Top right, ii), same as ~~Left~~i) except the record is a little bit more complicated over a tidal period. ~~Right: Same~~Bottom, iii), same as ~~Center.~~ii).

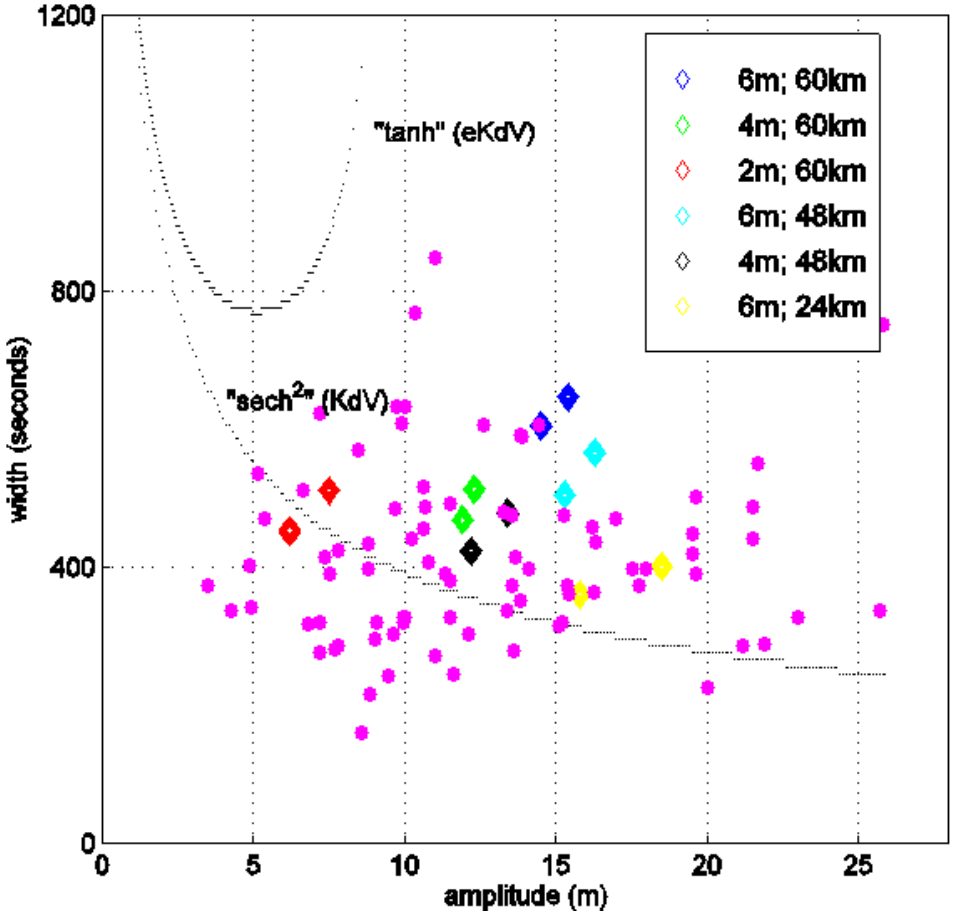

Fig. ~~20~~14. Wave amplitude vs. wave width at the CMO mooring for waves from all events during the period day 210 - 245. Also plotted are the two leading waves from six of the nine model runs shown in Fig. ~~16~~10 (diamonds).

Supplementary Figure

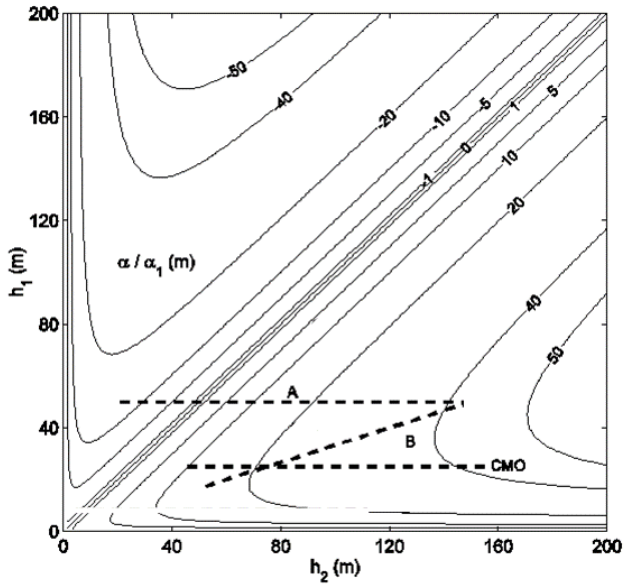

Fig. ~~Tables~~

~~Case~~	~~h_1~~	~~h_2~~	~~α/c~~	~~β/c~~	~~α~~	~~β~~	~~c~~	~~$(12\beta/\alpha)^{1/2}$~~
~~1~~	~~50~~	~~150~~	~~-.02~~	~~1250~~	~~-.0145~~	~~906~~	~~0.725~~	~~628~~
~~2~~	~~40~~	~~85.7~~	~~-.02~~	~~571~~	~~-.0124~~	~~353~~	~~0.618~~	~~362~~
~~3~~	~~80~~	~~93.8~~	~~-.0021~~	~~1250~~	~~-.0016~~	~~972~~	~~0.777~~	~~2041~~
~~4~~	~~65.1~~	~~115.1~~	~~-.01~~	~~1250~~	~~-.0076~~	~~954~~	~~0.763~~	~~1227~~

~~Table 1. KdV parameter values for Cases 1 – 4.~~

S1. Quadratic nonlinear parameter, α, divided by the cubic nonlinear parameter, α_1, as a function of the depth of the upper layer, h_1, and lower layer, h_2. Values for sloping bottom (Cases A and B) and realistic slope and stratification at the CMO site are shown by the broken lines.

Formatted: Normal

Formatted: Font: 12 pt